Université d'Ottawa · University of Ottawa

DEVELOPMENT OF REVERSE OSMOSIS LOW PRESSURE MEMBRANES

Gita G. Nurlaila

A thesis submitted to the School of Graduate Studies and Research
in partial fulfillment of the requirements for the
degree of
MASTER OF APPLIED SCIENCE
in the Department of Chemical Engineering
University of Ottawa

June 1997

Abstract

Thin film composite (TFC) membranes were developed for reverse osmosis (RO) under low pressure. Three commercial membranes, i.e. one type of polyvinylidene fluoride, namely AP-10, and two types of polyethersulfone, namely HW-18 and E-500, were used as substrate membranes. Sulfonated poly(2,6-dimethyl-1,4-phenyleneoxide), known as SPPO, was used as the ultrathin barrier layer of the composite membranes. The performances of the three substrate membranes were compared. The pore size and the pore size distribution of the substrate membranes were studied. Then the RO performances of the substrate membranes coated with SPPO were compared. It was observed that a high electrolyte separation without scarification of permeate flux was attained when membrane E-500 was used as the substrate membrane. Afterwards, the effects of the number of coating layers and the coating solution concentrations on RO performance of the TFC membranes, using E-500 membrane as the substrate membrane, were studied. The optimum coating solution concentration and the number of coating layers for maximum electrolyte separation were determined. The TFC membrane was then subjected to post-treatments, i.e. annealing and heat treatment under water, to improve the permeate flux. The final post-treated TFC membrane performance was concluded to be close to the targeted value.

Le Résumé

Les membranes pelliculaires composées (PC) ont été développées afin de traiter les déchets aqueux par osmose inverse à basse pression. Trois membranes commerciales ont servi de substrat: la première (AP-10) étant composée de fluorure de polyvinylidène et les deux autres (HW-18 et E-500) de polyéthersulfone. Le poly (2,6-diméthyl-1,4-phénylèneoxide) sulfoné, communément appelé SPPO, a formé la barrière ultra-mince des membranes composées. La performance des trois substrats a été comparée. La distribution et la taille des pores ont été étudiées. La performance sous condition d'osmose inverse des trois membranes recouvertes de SPPO a ensuite été comparée. La séparation électrolytique et la perméabilité de la membrane E-500 étaient maximales. L'effet du type de couche et du nombre de couches utilisées sur la performance des membranes PC sous condition d'osmose inverse a ensuite été mesuré. La concentration de SPPO ainsi que le nombre de couches qui permettent une séparation électrolytique maximale ont été déterminés. La membrane PC a ensuite subit des après-traitements (chauffage sous l'eau, fusion) afin d'améliorer sa perméabilité. La performance de la membrane PC prétraitée se rapproche de la valeur optimale.

Acknowledgement

The author would like to express her appreciation for the supervision and support provided by Dr. Takeshi Matsuura. Thanks are also due to Dr. Geeta Chowdhury for her assistance throughout this project, to Mr. Surendra Singh, Mr. Louis Tremblay and Mr. Frank Ziroldo for their technical assistance and support, and to all IMRI staff for their assistance and friendliness.

The author is very thankful to Zenon Inc. for their financial support throughout her studies and research. Thanks also due to Osmonics, Inc. for providing HW-18 UF membranes and to Department of Chemical Engineering, University of Ottawa, for its partial contribution of the financial support throughout the author's studies.

Special thanks go to Dr. Handan Tezel for her everlasting encouragement and support throughout the author's studies.

Finally, the author wishes to graciously thank the companionship and the full support provided by her husband, Gatot Susilo.

TABLE OF CONTENTS

List of Tables

List of Figures

NOMENCLATURE

a	Einstein Stoke Radius (ESR) (m).
$\underline{a}$	ESR of mean macromolecule (m).
$\tilde{A}$	constant characterizing electrostatic repulsion force (m).
$\tilde{B}$	constant characterizing van der Waals attraction force (m^3).
$\tilde{C}$	constant characterizing the repulsion force due to overlap of electron clouds (m^{12}).
C_f	solute concentration in feed stream (g/L).
C_p	solute concentration in product stream (g/L).
$\underline{d}$	distance between the membrane surface and the solute molecule (m).
$\tilde{D}$	constant characterizing steric repulsion at the interface (m).
D_w	radius of water molecule (m).
$\tilde{E}$	constant characterizing friction force (m)
f	solute separation (%).
R	pore radius (m).
$\underline{R}$	average/mean pore radius (m).
R	gas constant (J/mole.K).
R_a	effective radius of membrane pore available for fluid flow (m).
R_b	radius of membrane pore (m).
T	absolute temperature (K).

Greek Letters

Γ	surface excess of solute (mol/m^2).
γ	interfacial tension (N/m).
δ	pore length (m).
θ	dimensionless sieving coefficient.
σ	standard deviation.
σ_a	geometric standard deviation about mean ESR.
τ	dimensionless log normal distribution function.
Φ	dimensionless surface potential function.
Ψ	function of friction force restricting solute movement (m).

CHAPTER ONE

INTRODUCTION

1.1 Background

Separation has been a common process in human life for a very long time. In nature, a substance almost always exists in mixture with another substance. Thus, in order to use a particular substance, it has to be extracted from the mixture.

Although conventional separation processes, such as distillation, are still used in industries, more and more people are looking towards membranes for their separation technology. The history of membrane process development goes back to 1920, when Zsigmony introduces microfiltration as the first membrane process, followed by the introductions of ultrafiltration in 1930, hemodialysis in 1950, electrodialysis in 1955, reverse osmosis in 1960, gas separation in 1979, and pervaporation in 1982 (Mulder, 1992).

Loeb and Sourirajan first introduced reverse osmosis as an alternative in the desalination process in 1960. Since then, a lot of efforts were made towards the improvement of the reverse osmosis process for desalination and water treatment purposes.

1.2. What is a Reverse Osmosis Process

Osmosis is a process where the fundamental works lie on the diffusion of molecules through a semi selective thin layer, so-called membrane. Pure liquid molecules are transported through a membrane from the side of lower solute concentration to the side of higher solute concentration. Related to this process is the term osmotic pressure, which is defined as the differential hydrostatic pressure of the water level in the less concentrated side of the membrane and that in the more concentrated side.

When a pressure greater than the osmotic pressure is applied to the more concentrated side of a membrane, a flow of pure liquid molecule is reversed, i.e. from the more concentrated side to the less concentrated side of the membrane. This process is called Reverse Osmosis, or briefly, RO (Matsuura, 1994).

The main purpose for the development of RO membranes has been for desalination and water treatment. Research conducted by Loeb and Sourirajan on development of RO membrane opened a new window of limitless research ideas for reverse osmosis processes and membrane developments for reverse osmosis process. Since its first introduction in 1960, a lot of effort has been focused on finding membranes with economical values, that is, having an acceptable permeation flux with a desired salt separation. Accordingly, more methods and modifications in preparing membranes have been invented, including crosslinking, heat treatment, thin film composite and others. One of the methods mentioned was actually carried out in this work, that is the thin film composite method or TFC.

1.3. Thin Film Composite Membrane

Theoretically, according to Petersen (1993), a thin film composite RO membrane may be defined as a bilayer film formed by a two step process. The first layer is usually made of a thick, porous, non-selective layer formed in the first step. This layer is also referred to as the microporous support film. The layer is subsequently over-coated with an ultrathin barrier layer on its top surface in the second step. The top layer can also be referred to as the ultrathin dense layer. Usually the two layers are different from one another in chemical compositions.

In practice, however, a TFC membrane consists of three layers, where the bottom layer only functions as a support and a preventor of the membrane damaging process from a rough surface. The bilayer film mentioned in the Petersen's theory is actually the middle and the top layer of a TFC membrane.

The purpose of using a composite membrane rather than using a regular asymmetric membrane is that the ultrathin barrier layer (the top layer) in a composite membrane provides the controlling properties as to semi permeability, whereas the microporous support (the middle layer) provides the necessary strength and better solvent flux. Each individual layer can thus be optimized separately for its particular function. The combination of the two layers is expected to give a maximum performance of a membrane, i.e. high separation and high flux. In an asymmetric membrane, this may not be done since an asymmetric membrane has the ultrathin layer integrally supported by a porous underlayer. The material of the former layer is the same as that of the latter layer and the membrane is made in a one step process.

A typical composite RO membrane as commercially produced is shown schematically in Figure 1.

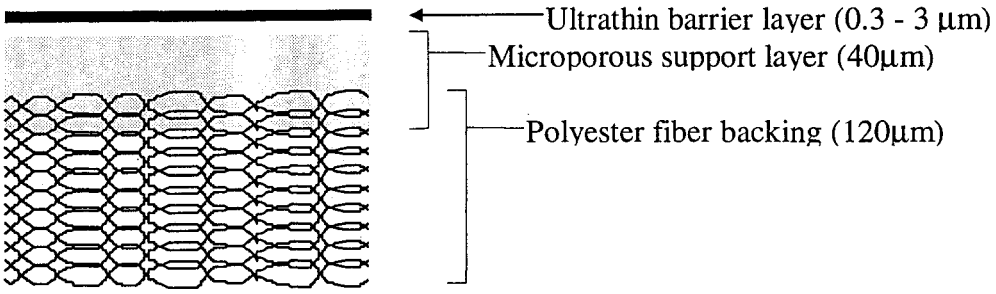

Figure 1. A Typical Schematic of RO Thin Film Composite Membrane

Here the microporous support film (the middle layer) is cast on a woven or non woven backing material, usually made of polyester fibers. The support is approximately 40μm in thickness and about half of it penetrates into the polyester backing material. The polyester web structure, which is comprised of the polyester backing material and the microporous support layer, is usually employed without drying for applications of the reagents used to form the ultrathin barrier layer. After deposition of the barrier layer (the top layer), the composite membrane is subsequently dried and/or heat cured to complete the membrane preparation (Cadotte and Petersen, 1981). In instances where the thin barrier layer (top layer) is not strongly attached to the support surface (middle and bottom layers), drying may form an adequate bond. Generally it is preferred that the ultrathin barrier layer is well bonded to the microporous support surface to prevent damage or delamination during use.

More often than not, the microporous support layer does not have to be directly coated onto a fabric base. Instead, it can be cast onto a glass plate separately and is then over coated

with ultrathin barrier layer of polymer solution (Petersen, 1993). When membrane is ready to be tested, the bilayer composite membrane is simply placed on a sheet of the polyester backing material for structural support during mounting in the test cells. Another method is by using a filter paper. A RO test cell usually consists of a porous sintered metal plate that comes under the membrane. The filter paper placed between the membrane and the metal plate prevents the membrane from touching the rough surface of the metal plate.

The disadvantage of using a composite membrane is that manufacturing a composite membrane is more expensive than manufacturing an asymmetric membrane. However, for a majority of reverse osmosis applications, the extra cost of manufacturing a composite membrane is more than counterbalanced by the improved performance characteristics of the resulting membrane products.

In the development of the thin film composite method, there were two groups of researchers: one group was using cellulosic membrane as the substrate membrane and the other was using non-cellulosic membrane as the substrate membrane. The former group usually consisted of those who conducted the thin film composite experiments in earlier years while the latter group consisted of those of later years.

The origin of thin film composite (TFC) reverse osmosis membrane can be attributed to Peter S. Francis in 1964 (Petersen, 1993). In the case of Francis membranes, the ultrathin dense barrier layer and the porous substructure of the asymmetric membrane were separately fabricated and then laminated together. On the other hand, the asymmetric films of Loeb-Sourirajan membranes have an ultrathin, dense, surface barrier layer integrally supported by a thick, porous, and spongy underlayer.

Francis (1966) made his TFC membrane, using float cast on a water surface method. The ultrathin film was made by float-casting a liquid film of cellulose acetate solution in cyclohexane onto a water surface. Migration of the cyclohexane from the organic phase into the aqueous phase left behind a floating skin of cellulose acetate on the water. The ultrathin film of a candidate polymer was laminated to a microporous support layer by sliding an appropriate microporous support under the water surface and bringing it underneath the floating film.

The thickness of the dense barrier film in Francis' membrane was able to be controlled to within 15% over the range of 200 to 5000 A ($2x10^{-8}$ to $5x10^{-7}$ m). However, the composite membranes were found to have relatively low surface porosity and low permeation rate of 2-3 gallon per square foot per day (gfd) or $8.72x10^{-6}$ - $1.31x10^{-5}$ $m^3/m^2.s$ at 1500 psig pressure (10.3 MPa gauge) due to compaction. Severe pressure compaction of cellulosic membranes was just beginning to be recognized as a major flux limiting phenomena in the development of the TFC membranes.

Riley et al. (1964) introduced an alternative method of fabricating the thin film composite membrane using a meniscus coating method. The method was basically a one sided dip-coating procedure where the membrane is prepared by directly forming a very thin film of a polymer, generally cellulose triacetate, upon the finely porous surface of a supporting membrane. The approach was still using mixed cellulose esters as microporous support.

Rozelle et al. (1967) compared the performances of composite membranes with microporous non-cellulosic support films made from polysulfone, polycarbonate, and PPO. The ultrathin membrane used in the work was cellulose acetate. Of these, polysulfone

proved to have the best combination of compaction resistance and surface microporosity. The membrane showed an increase in flux from 2-3 gfd in the previous research done by Francis to about 10-15 gfd or 4.36×10^{-5} - 6.54×10^{-5} at 1500 psig (10.3 MPa gauge). Since then, microporous polysulfone has been widely used as the support film in composite membranes.

In 1970, Rozelle et al. discovered NS-100, a membrane containing an ultrathin aryl-alkyl polyurea, which was formed on a microporous polysulfone support (Cadotte and Petersen, 1981). This membrane demonstrated qualities that are promising for seawater desalination. Two important characteristics that resulted were non-biodegradability and no compaction under sustained high-pressure (Rozelle et al., 1977). The membrane was fully non-cellulosic, having no cellulose ester polymers in either the ultrathin barrier layer or the microporous support layer. Since that time, most TFC membranes have been non-cellulosic.

Riley et al. (1971) also made another attempt to produce composite membranes for seawater desalination using reverse osmosis. However, cellulose acetate was still used as the support layer. Based upon their previous success in increasing the flux by making a thinner barrier layer (Riley et al., 1964), the approach this time used a barrier layer with a thickness of 400 A (4×10^{-8} m). The composite membrane was prepared by directly forming a very thin film of a polymer, generally cellulose triacetate, onto the surface of a supporting membrane. Using only 2.7 atm gauge (0.27 MPa gauge) operating pressure, the membranes were capable to have fluxes in excess of 12 GFD (5.23×10^{-5} $m^3/m^2.s$) with sodium and

chloride ion rejections ranging from 99.45% to 99.62%. While proven to be feasible, this approach was overtaken by a new development of non-cellulosic composite membranes.

To summarize methods which have been used for fabricating composite reverse osmosis membranes, Cadotte and Petersen (1981) listed five major routes:

1. Cast an ultrathin dense membrane film separately, then laminate to a microporous support. This is the method used in Francis' approach.

2. Dip coat a polymer solution onto a microporous support film followed by drying. This method was first used in Riley's approach.

3. Dip coat a solution of a reactive monomer or prepolymer onto a microporous support, followed by a post-cure with heat or irradiation.

4. Deposit a barrier film directly from gaseous phase monomer plasma onto the support film.

5. Interfacially polymerize a reactive set of monomers at the surface of the support film.

1.4. Charged Composite Membrane

Since some of feed solutions to be separated are electrolyte solutions, it would be best to have a charged membrane. Thus, the separation, which is initially due to the pore size of the membrane (size exclusion), is now enhanced by the presence of charge on the surface

of the membrane (charge exclusion). In fact, the electric repulsion exerted by a charged membrane largely contributes to the high separation of electrolyte feed solutions.

Referring back to the history of the development of charged membranes, bentonite clay may be considered the first material used as a charged membrane. Kemper and Maasland (1964) first used this material, acting as the semiselective layer, to investigate the reduction in salt content of solution on passing through thin films adjacent to charged surfaces ions. Using feed solutions of sodium chloride and calcium sulfate, the result showed that salt sieving generally increased as the pores through which the water flew decreased in size and was less when the soil was saturated with divalent rather than monovalent ion.

Similar conclusion was obtained by Rolfe and Aylmore (1981), who conducted a study on electrokinetics and salt sieving properties of compacted clays. Using Wyoming bentonite and Willalooka illite cores as the semiselective layer, they also observed that feed containing monovalent ions gave higher rejection than feed containing divalent ions. The highest separation achieved in the research was 73% when feed containing 0.0174 M NaCl was used.

In charged composite membranes, the selectivity performance is mainly controlled by the electric charge of the ultrathin layer of the membranes. The ionic group of the charged ultrathin layer exerts a repulsive force to ions of electrolyte feed solutions having the same charge as the ions of the ultrathin layer. The repulsion working on a charged composite membrane is effective over a range longer than the dielectric repulsive force working between ions and a neutral surface. Thus, a charged composite membrane having a larger

pore size can achieve the same level of rejection of electrolyte solutes given by a neutral membrane having a smaller pore size.

As a result, a charged composite membrane can reject ions much smaller than its pore radii. However, solutes with no electric charge are rejected less efficiently and hence, a charged composite membrane cannot reject solute with no electric charge having a size smaller than its pore radii (Nakao et al., 1988; Jitsuhara and Kimura, 1983).

Charged thin film composite membranes were reported to have high permeation rates and high resistance to chlorine, together with ability to operate under wider pH ranges and high temperature (Agarwal et al., 1988 and Ikeda et al., 1988). High permeation rates can be obtained due to the thickness of the ultrathin layer of a composite membrane that is much smaller than the thickness of an asymmetric membrane. The high permeation rates also mean that a charged composite membrane can be operated at a lower operating pressure (Kurihara et al., 1985).

Since the charge in a charged composite membrane is normally negative, electrolyte solutes with higher anionic charge densities or with lower cationic charge densities are rejected more effectively.

Sata et al. (1979) observed that a cationic polyelectrolyte layer narrowed the pathway for ions in a charged composite membrane. Surprisingly, the cation with larger hydrated diameter (potassium ions) was found to permeate more easily through the charged composite membrane having a polyelectrolyte layer than that with the smaller hydrated diameter (sodium ions). Lower valent cations (in this case Na^+ and K^+) are more selectively

permeated through the charged composite membrane than higher valent ones (in this case Ca^{2+}). This confirms the findings in the previous works using clays. In Sata's work, polyethyleneimine was used as the cationic polyelectrolyte layer with NEOSEPTA CL-25T used as the microporous support.

Sata and Izuo (1990) studied the electrodialytic properties of charged composite membranes. An ultrathin layer of polyethyleneimine, bonded to the microporous support layer by acid-amide bonding, covered styrene-divinyl benzene, which was used as the microporous support layer of the composite membrane. Due to the charge nature of the polymer used, the membrane is considered a cation exchange membrane. Using 2.5 N NaCl as the feed solution, it was observed that monovalent cation permselectivity decreased gradually during the electrodialysis in the cation exchange membrane. They also found that crosslinking reaction of polyethyleneimine was proven to be more effective than alkylation in maintaining the high permselectivity constantly.

Modification from a neutral composite membrane to a charged composite membrane can be done by electrophilic substitution reactions, such as bromination, acetylation, sulfonylation and sulfonation.

Tsuru et al. (1991) analyzed the reverse osmosis of single and mixed electrolytes with charged membranes made of polysulfone coated by sulfonated polyethersulfone. Due to the nature of sulfonated polymer, the composite membrane made was negatively charged. Experimental result showed that rejection by the charged composite membrane was strongly dependent upon feed concentration. Lower feed concentration yielded higher rejection, whereas higher feed concentration yielded lower rejection. It was observed that

rejection of electrolytes having divalent coion (SO_4^{2-}) was much higher than that of electrolytes having monovalent coion (Cl^-). On the other hand, electrolytes having monovalent counterion (Na^+, K^+) showed higher rejection than those having divalent counterion (Mg^{2+}, Ca^{2+}).

Percec (1987) studied the chemical modification of PPO by electrophilic sulfonylation and acylation of the aromatic structural units. It was observed that the maximum monosubstitution degree of PPO was 79.4 while higher substitution levels were difficult to achieve due to a decrease in nucleophilicity and steric hindrances of the remaining position. Compared to the parent PPO, minor changes in thermal stability and a broadening of the solubility range of substituted PPO were recorded. Very good permeation (both permeability and selectivity) properties to gases, better than PPO, were detected for the modified structure.

1.5. Donnan Exclusion Theory

In 1911, F.G. Donnan first elucidated the behavior of a membrane that is impermeable to a particular ionic species in the solution. The equilibrium in the system can be described as the following:

solution phase	**membrane phase**
A^+, Y^-, H_2O	A^+, Y^-, R^-, H_2O

Figure 2. Description of Donnan Equilibrium

Here, the equilibrium is established between the solution phase AY (on the left side) and the membrane phase AY + AR (on the right side). In the system, one ionic species (the fixed ionic group, or the R^- ions) is fixed to the membrane phase. To his honor, such membrane equilibria are called "donnan equilibria" and the electric potential differences between the two phases are called "donnan potentials". Because of the analogies, the term donnan equilibrium and donnan potential are now also applied to sorption equilibria of strong electrolytes and phase boundary potentials between ion exchangers and solutions.

Helfferich (1962) described the donnan potential and donnan equilibrium for ion exchangers quite extensively. A cation exchanger, which is placed in a dilute solution of a strong electrolyte, creates a considerable concentration differences between the two phases. The cation concentration is larger in the ion exchanger while the (mobile) anion concentration is larger in the solution. Migration of cations into the solution and migration of anions into the ion exchanger result in an accumulation of positive charge in the solution and of negative charge in the ion exchanger. The first few ions that diffuse thus build up an electric potential difference between the two phases. This so-called "donnan potential" pulls cations back into the (negatively charged) ion exchanger and anions back into the (positively charged) solution. Equilibrium is established in which the tendency of the ions to level out the existing concentration difference is balanced by the action of the electric field. In the ion exchanger, the counter ion (cation) concentration thus remains much higher and the co-ion (anion) concentration much lower than in the bulk external solution. Analogy of this phenomenon to a charged membrane performance is established by replacing the cation exchanger with the charged membrane.

The donnan potential has one immediate consequence for electrolyte sorption: it repels co-ions from the charged membrane and thus prevents co-ions from being sorbed by the membrane. Co-ion uptake and electrolyte sorption are equivalent because of the electroneutrality requirement. Hence, the electrolyte is, at least partially, excluded by the charged membrane.

The higher the donnan potential (in absolute value), the stronger is the exclusion, i.e. the smaller is the electrolyte uptake. Donnan potential, in turn, depends on the ionic concentration and charge. Equilibrium is attained when the action of donnan potential balances the tendency of the counter ions to diffuse out into the solution. The effect of electrolyte exclusion increases with decreasing solution concentration and with increasing capacity of the charged membrane.

The force with which an electric field acts on an ion is proportional to the ionic charge. Hence, donnan potential that is required to balance the tendency of the counter ions to diffuse into the solution is smaller when the valence of the counter ions is higher. Because of the smaller donnan potential, electrolyte exclusion is less efficient. On the other hand, a given donnan potential excludes the co-ions more efficiently when the co-ion valence is higher. Consequently, electrolyte exclusion is more efficient with counter ions of low valence and co-ions of high valence. For example, Na_2SO_4 is more strongly excluded by a cation exchanger than NaCl, and NaCl is more strongly excluded than $CaCl_2$. For an anion exchanger, the sequence is the opposite.

In 1970, Plummer et al. observed the dependence of RO performance of a polypropylene membrane coated with SPPO solution on feed composition. The feed compositions used

were $MgSO_4$, $MgCl_2$, NaCl and Na_2SO_4. The observation revealed that electrolyte rejection for $MgSO_4$ is higher than for $MgCl_2$ and the rejection for NaCl is higher than for $MgCl_2$. These findings confirmed the theory mentioned above.

1.6. Membrane Material

The major purpose of using thin film composite structure in this work is to have a high permeation flux while maintaining a high salt separation. Thus, the main criteria for selecting the material for the ultrathin layer is a high salt separation characteristic, whereas the criteria for selecting the support film is a high permeation feature.

General requirements in the selections of membrane materials for wastewater treatment are listed below:

1. The membrane has to be stable at high temperature (approximately higher than 80°C).

2. The membrane has to be stable at high or low pH. This is to take into account any acidity or basisity which may exist in wastewater.

3. The membrane has to be economical in price and be available in a large quantity to assume the continuity of the wastewater treatment.

4. The membrane has to have good mechanical strength and be durable for a long period of time (usually 3 years) to avoid plant's downtime and thus, reducing operating cost of the plant.

Among the commercial membranes available, polyvinylidenefluoride, or PVDF, and polysulfone, or PS, were considered to be the most appropriate candidate for the microporous support layer. These commercial membranes were also referred to as substrate membranes. As the ultrathin barrier layer, poly (2,6-dimethyl-1,4-phenylene oxide), or PPO, was chosen for its thermal stability. The following provides a detailed description of each polymer used.

1.6.1. Polyvinylidene fluoride

Polyvinylidenefluoride (PVDF) is very stable to harsh chemical, thermal, ultraviolet, weathering, and oxidizing or high-energy radiation environments (Dohany and Humphrey, 1985). It is considered as tough engineering thermoplastics due to its high thermal degradation temperature (390°C) and high heat-deflection temperature.

Compared to other perfluorinated polymers that are of high temperature resistance as well, PVDF has excellent resistance to elastic deformation under load (creep), repeated flexing, or fatigue. The resistance to abrasion by a variety of tests is excellent, especially considering the relatively high hardness value (Hertzberg and Manson, 1980).

Polyvinylidenefluoride is prepared by methods that assure exceedingly low contamination and does not require additives for stabilization. Therefore, it is an excellent material for applications where high purity is demanded for materials of construction, such as ultra pure water systems (Dohany and Humphrey, 1985).

Another advantage of polyvinylidenefluoride is that it exhibits an exceptional resistance, even at elevated temperatures, to most inorganic acids, halogens, oxidants, weak bases and

aliphatic, aromatic, and chlorinated solvents. However, strong bases, amines, esters, and ketones cause swelling, softening, and dissolution, depending on conditions (Dohany and Stefanou, 1975).

Because it is resistant to many chemicals and is approved by the Federal Drug Administration for food contact, the chemical and the food industries are using PVDF filters and fluid-handling systems. Polyvinylidenefluoride sheets supported with woven glass or polyester fiber are used in chemical tank linings for corrosion protection (Dohany and Humphrey, 1985).

Because of its unusually high dielectric constant property, polyvinylidenefluoride has applications in many specialized uses requiring high performance thermoplastic properties and fluoroplastic attributes. It is used as a primary insulator on computer hookup wire in computer back panels (Dohany and Humphrey, 1985).

1.6.2. Polysulfones

Polysulfones (PS) are clear, rigid, tough thermoplastics with glass transition temperature (Tg) of 180-250°C (Harris and Johnson, 1985). Chain rigidity in the polymer is originated from the relatively inflexible and immobile phenyl and SO_2 groups, and toughness from the connecting ether oxygens. These groups also contribute to the thermal stability and chemical inertness that characterize the polymer. Those properties, along with the high glass-transition temperatures, make possible continuous use in the 150-200°C range. Polysulfones exhibit excellent resistance to burning and, in most applications, require no flame-retardant additives.

Polysulfones and polyarylethers, in general, have excellent hydrolytic stability compared to polycarbonates, polyesters, and polyetherimides and may undergo many hours of exposure to hot water and steam (Robeson and Crisafulli, 1983). Within a broad range, pH has little effect on the rate of hydrolysis and, consequently, polysulfones are highly resistant to aqueous mineral acid, alkali, and salt solutions.

As with all amorphous glassy polymers, polysulfones exhibit stress cracking and crazing in organic solvents. An important variable in determining environmental stress craze resistance (ESCR) is the solubility parameter. Cracking or crazing (qv) occurs at low stress-strain if the solubility parameter of the environment and the polymer are within 1-2 units of each other (Kambour et al., 1972). Polyphenylsulfone, polyarylethersulfone, and polyethersulfone, all with solubility parameters above 22 $(J/cm^3)^{1/2}$, are more resistant to aromatic hydrocarbons, esters, ketones, and some chlorinated aliphatic hydrocarbons (Hay, 1969[b]). Thermal (physical) aging properties and solvent crazing or cracking (qv) resistance of molded articles can be improved by annealing, which relieves stresses and increases stiffness. However, over-annealing can reduce impact resistance.

The solubility of polysulfones in common solvents ranks according to bisphenol A polysulfone > polyarylethersulfone > polyethersulfone > polyphenylsulfone (Harris and Johnson, 1985). All are completely soluble in polar solvents such as dimethylformamide and N-methylpyrrolidinone (NMP) as might be expected from their solubility parameters.

In contrast to many other polymers, the melt viscosities of polysulfones are insensitive to shear (Harris and Johnson, 1985). Although not highly shear-sensitive, the viscosities of polysulfones are highly temperature-sensitive.

One disadvantage of having polysulfone as the polymer for the membrane substrate is that it has a hydrophobic character. This may cause problem, especially if the membranes are allowed to partially dry out after usage.

Due to solvent sensitivity of the polymer, a careful selection of the type of polysulfone to be used as the microporous support may have to be employed as problems may arise when modification such as thin layer coating is to be done on the membrane. The selection of solvent-based coating solution for thin film composite membrane may also be narrowed in some extent. Polyethersulfone (PES) was used in this work since it has better environmental stress cracking resistance compared to other polysulfones.

1.6.3. Poly(2,6-dimethyl-1,4-phenyleneoxide)

Poly(2,6-dimethyl-1,4-phenyleneoxide), or known as PPO, is an amorphous polymer known for its high Tg (glass transition temperature), excellent mechanical properties and resistance to a number of chemical agents and is proven to be a highly permeable membrane material.

PPO has a glass transition temperature of 212°C and thus belongs to the class of thermally stable engineering plastics. It is also reported as having a good thermal stability under non oxidizing conditions (Petersen, 1993). Fu et al. (1994) reported that the initial decomposition temperature for this polymer is 470°C at a heating rate of 10°C/min, which is the result of the splitting of the main chains.

PPO is also known to be hydrophobic. A measure of its hydrophilicity is given by the contact angle of a homogeneous PPO film which was found to be 67°. As a comparison,

contact angle for cellulose acetate (CA) was measured to be 32°, whereas that for polyethylene film was 95°. Although solubility of water in PPO film is only one-tenth that of cellulose acetate (CA), the diffusivity of water vapor through PPO film is about six times as much as CA film (Fu et al., 1994).

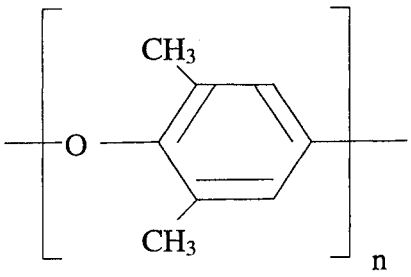

Figure 3. Structure of Poly (2,6-dimethyl-1,4-phenyleneoxide)

A large number of modification reactions on PPO to improve its properties has been reported in the literature. Cabasso et al. (1974) carried out benzylic substitution of PPO with pendant phosphate groups. Verdet and Stille (1982) studied the attachment of cyclopentadiene ligands to PPO, followed by their conversion of η-cyclopentadiene with cobalt, modium, and titanium together with the catalytic reactions of these polymer-supported complexes. Percec et al. (1983) prepared a high molecular weight comb-like PPO from PPO-styrene macromonomer via radical homopolymerization and copolymerization. The carboxylation of PPO using lithiation method followed by treatment with CO_2 as well as further modification to form various carboxylate derivatives such as esters, salts, amides, anhydrides, etc. and their miscibility behavior in different blends was also reported (Xie et al. 1968).

1.7. Composite Membrane Having Sulfonated Poly(2,6-dimethyl-1,4-phenyleneoxide)

Introduction of sulfonated composition to the poly(2,6-dimethyl-1,4-phenyleneoxide), or PPO, polymer is one way to make a charged membrane. A large solubility coefficient for water of sulfonated PPO is caused by highly hydrophilic nature of sulfonic acid. Therefore, it may help to produce a high pure water permeation (PWP) rate in composite membranes. Sulfonated asymmetric membranes have been known in the 1960s and were made from sulfonated poly (2,6-dimethyl-1,4-phenyleneoxide) (Sourirajan, 1977).

Sulfonation and sulfation are chemical methods for introducing the SO_3 group into organic entities (Hay, 1969[c]). In sulfonation, an SO_3 group is introduced into an organic molecule, to give a product with $-SO_3-$ linkages (sulfonates) in the form of a sulfonic acid ($-SO_3H$), a salt ($-SO_3Na$), or a sulfonyl halide ($-SO_3X$) (Standen, 1968).

Sulfonation and sulfation processes have been widely used in industry. The introduction of a sulfonic acid group into a specific position in an aromatic nucleus and the subsequent substitution of a hydroxyl group by alkali fusion represent a basic industrial process. In another application, a sulfonated emulsifier will concentrate at the interface between oil and water phases and thus, contributing to a stable emulsion. In a broader sense, sulfonation and sulfation processes provide the means to interface with, modify, or bridge aqueous and organic systems. This principle is used in the development of water-dispersible or water-soluble dyes, flavors, and medicines by introducing the water-solubilizing sulfonate group.

In 1960s, sulfuric acid was the only known sulfonating reagent; today, it and oleum are the most widely used reagents because of their convenience and low cost. Chlorosulfonic acid, usually employed in stoichiometric amounts, is another important low cost sulfonation reagent. It does, however, suffer from two drawbacks namely, its corrosive nature and the fact that it reacts with evolution of hydrogen chloride, which presents a disposal problem. Alternatively, the hydrogen chloride may be absorbed in a water scrubber and sold as a commercial grade or recycled.

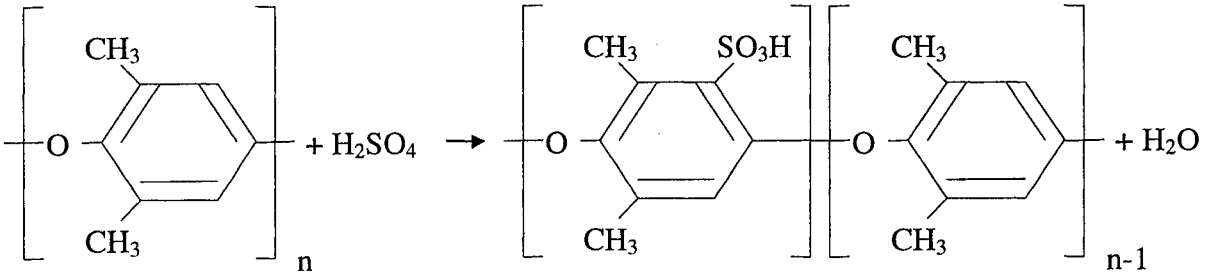

Figure 4. Sulfonation of Poly (2,6-dimethyl-1,4-phenyleneoxide) using Sulfuric Acid as Sulfonating Agent

Although sulfuric acid-based sulfonation processes continue to dominate, SO_3 based processes have increased significantly over the last 15 years, including the development and utilization of continuous SO_3 film sulfonation and sulfation processes.

Stabilized liquid sulfur trioxide, introduced commercially as a sulfonation/sulfation reagent in 1947, is second only to oleum (Schnoor and Yodis, 1964). Because of its extreme reactivity, special handling and processing methods are required in order to avoid overreaction, oxidation, and charring.

Economic considerations heavily influence the choice of reagent. Although both sulfuric acid and oleum are cheaper than SO_3, a large excess of both reagents is required, which creates substantial quantities of spent acid that have to be discarded or recycled, and affects the economics of the process. In contrast, SO_3 and chlorosulfonic acid usually react stoichiometrically to give products containing very little sulfuric acid; consequently, the neutralized product contains only small amounts of sodium sulfate.

Fu et al. (1994) did two sulfonation reaction types on PPO polymer, i.e. one using sulfuric acid as the sulfonating agent and the other using chlorosulfonic acid as the sulfonating agent. It was observed that sulfonated polymer from chlorosulfonic acid had a relatively high sulfonation degree compared to that from sulfuric acid. The extent of the reactions was observed to be controlled mainly by the reaction temperature and reactant ratio (molar ratio of $ClSO_3H$ to PPO). Reaction carried out at 0^oC had lower sulfonation degree compared to that of room temperature even though reactant ratio was high and reaction time was long. For isothermal reactions, higher reactant ratio yielded higher sulfonation degree. However, sulfonation could hardly exceed 40% due to the limited solubility of sulfonated PPO in chloroform.

It was observed that solubility characteristics of SPPO were completely different from those of PPO. While PPO was insoluble in dipolar aprotic solvents, such as dimethyl-sulfuric-oxide (DMSO), dimethylfluoride (DMF) and dimethylacetamide (DMAc), SPPO became soluble. This is very important because these solvents are conventional solvents used for casting asymmetric membranes.

From the analysis of wide angle X-ray diffraction (WAXD) of SPPO and PPO, Fu and colleagues found that intermolecular distance remained constant but density was increased after sulfonation. It means that packing of polymer chains became denser after sulfonation.

Fu and colleagues also found that the glass transition temperature (Tg) increased after sulfonation which indicated that segmental motion of polymer chains decreased as a result of the increased interaction between polymer chains caused by introduction of SO_3H group.

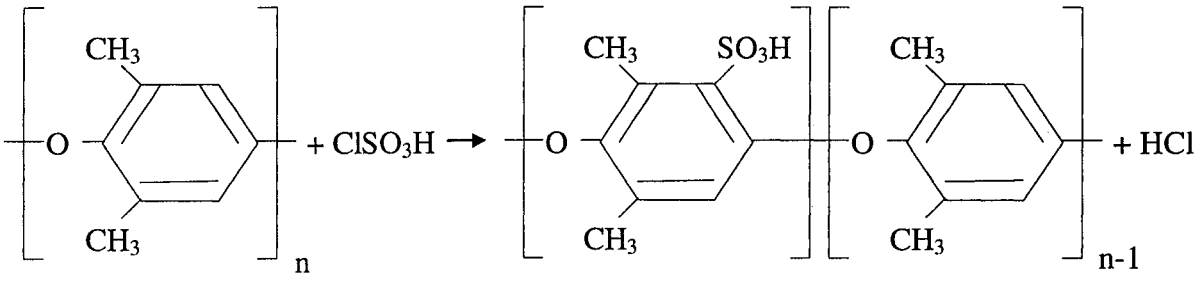

Figure 5. Sulfonation of Poly (2,6-dimethyl-1,4-phenyleneoxide) using Chlorosulfonic Acid as Sulfonating Agent.

In the sulfonation reaction of PPO polymer (refer to Figure 5), the SO_3H from the chlorosulfonic acid replaces the H from the aromatic ring of PPO. It is the SO_3^- ion which acts as a negative charge on the membrane to improve the selectivity of the electrolyte solution coming as a feed. The greater the negativity of the ion, the more it will be rejected by the SPPO layer.

Schauer et al. (1986) studied the preparation of ultrafiltration membranes from SPPO. PPO was sulfonated with concentrated sulfuric acid in the homogeneous phase. Variation in the degree of sulfonation showed that with increasing hydrophilicity of the polymer, the flow

rate of water through the membrane markedly increased. Increase in polymer concentration increased solute rejection when dextran was used as feed solution.

Chowdhury et al. (1994) studied different cationic forms of SPPO membranes. Comparison was made between sulfonate in hydrogen form (SPPO-H) and sulfonate in alkali metal salt form (SPPO-Me). Permeation rate was observed to be greater than pure water permeation (PWP) rate when the sulfonate was in the hydrogen form and the feed solution contained an alkali metal chloride solute. Also in this case, an increase in the ionic radius of alkali metal cation yielded an increase in the permeation rate.

When sulfonate was in the salt form, PWP increased with a decrease in ionic radius of alkali metal cation. Using operating pressure of 1 MPa and operating temperature of 25°C, NaCl separation for SPPO-H was observed to be 86.5% with PWP = 62.6 $x10^{-3}$ $g/m^2.h$ and PR (permeation rate) = 76.8 $x10^{-3}$ $g/m^2.h$ when the feed concentration was 0.01 mol/L. For SPPO-Na, NaCl separation was found to be 67% with PWP = 83 $x10^{-3}$ $g/m^2.h$ and PR = 89.6 $x10^{-3}$ $g/m^2.h$, when using feed concentration of 0.04 mol/L and operating conditions similar to that of SPPO-H.

Hamza et al. (1995) studied different ion exchange capacities (IEC) of SPPO membranes. They observed that there was a decrease in solute separation (78% to 65%) from IEC value of 1.29 to 1.98 and an increase (65% to 70%) from IEC value of 1.98 to 2.60. Product rate was found to be maximum (15.5 $x10^{-6}$ $m^3/m^2.s$) at IEC value of 1.98 when operating pressure was 1 MPa.

1.8. Ion Exchange Capacity Value

Sulfonation degree is expressed as the average number of - SO_3H (or - SO_3Na) groups in 100 repeating units of polymer. It could be determined using Dionex 2120I ion exchange chromatography (Hay, 1969[c]). The sulfonation degree is also often expressed as the Ion Exchange Capacity (IEC) value. This value gives information on how many -SO_3H ion replaces the H from the PPO aromatic ring. The greater the IEC value of a sulfonated polymer is, the more amount of -SO_3H ion had replaced the -H from the PPO aromatic ring. This also means that the negative charge on the polymer will be stronger and thus, the rejection on salt solution feed will be higher.

At low range of IEC values, SPPO is soluble in high chloroform/low methanol mixtures. At high IEC values, the polymer tends to be completely soluble in methanol alone. Also at high IEC values, the polymer swells excessively when treated with water. As observed by Plummer et al. (1969), increasing the IEC value of sodium form SPPO membranes from 1.19 to 2.03 increased the water content in the membrane from 40.9% to 80.3%. Increasing it further to IEC value of 4.45 resulted in water content of 264%, showing that the membrane is extremely swollen.

The SPPO used in this project had an IEC value of 1.87 meq/g dry polymer. The IEC value was chosen to be the optimum value for the separation. Increasing the value will mean the polymer will swell, while decreasing the IEC value will mean less rejection.

1.9. Changing from SPPO-H form to SPPO-Na form

Because of its electrolyte property, a charged membrane may change its chemical formation and eventually loses its IEC value. The major contributor to this chemical formation change is H^+ ion from SO_3H since it is very reactive. SPPO-H can be readily hydrolyzed according to:

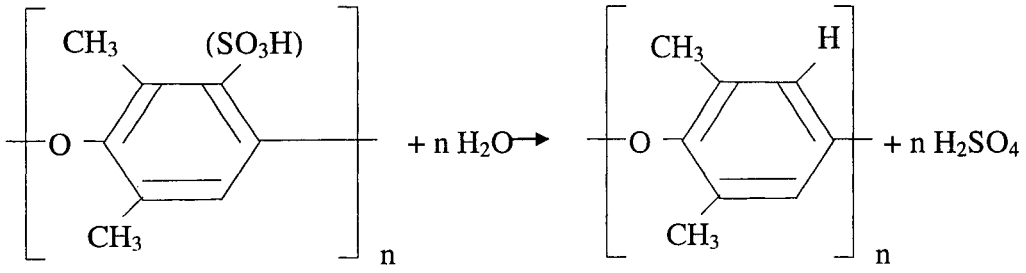

Figure 6. Hydrolysis of SPPO-H (Chludzinski et al., 1971)

This occurs rapidly at high temperature and somewhat at room temperature as long as some water is present. Thus, to maintain its chemical formation and preserve its IEC value, SPPO is changed from hydrogen form (SPPO-H) to sodium form (SPPO-Na). As salt of sulfonic acids, SPPO-Na are very stable to hydrolysis even at a temperature up to about 80°C (Plummer et al., 1969).

Fu et al. (1994) did a comparison between SPPO-Na and SPPO-H. They observed that the decomposition temperature of SPPO-Na is higher than that of SPPO-H. This shows that SPPO-H is unstable and acid-catalyzed degradation is likely to occur. The initial decomposition temperatures of both forms of SPPO are lower than that of PPO due to the

side group splitting (lower than 310°C). The main chain splitting temperature is also slightly lower than that of PPO. It was concluded that the thermal stability of PPO was decreased after sulfonation.

They also observed that water vapor permeability of SPPO in free-acid form was larger than that in sodium salt form at comparable sulfonation degree. The reason is that H-bonds are easily formed between the sulfonic groups in SPPO-H and water molecules, and leads to a greater hydrophilicity than for SPPO in sodium-salt form. It can be concluded that SPPO-H has higher permeability of water vapor.

From all the works involved in the literature survey, it was found that very little work was done for achieving a high permeate flux with a $MgSO_4$ separation greater than 90% at a low operating pressure. Moreover, only minimum discussion was conducted on the correlation of the pore size and the pore size distribution of the membrane to the electrolyte separation of thin film composite membranes carrying a charge.

1.10. Scope of Research

The research was conducted on commercially available ultrafiltration membranes that were high temperature resistant. They were used as microporous substrate membranes for the preparation of TFC membranes. A thin film of SPPO polymer was coated on top of the substrate membranes to render them ion-exchangable.

Furthermore, commercial membranes made of polyethersulfone (PES) and poly(vinylidene fluoride) (PVDF) were chosen to be substrate membranes since both are known for its high temperature resistance. To achieve the high salt separation requirements, modifications

were done on the membranes. In this case, a method called thin film composite method was used. This method is a process whereby an ultrathin barrier layer, which has a good selectivity on both $MgSO_4$ and NaCl, is placed on top of a commercially available membrane. It was expected that the permeation of the substrate membrane be maintained while attaining the high salt separation characteristic from the ultrathin layer that was placed on top.

1.11. Objective of Research

The purpose of this project is to develop a reverse osmosis membrane operable at low pressure about 150 psig (1.02 MPa gauge) and at high temperatures (>80°C). The membranes should further satisfy the following requirements to be considered economical for industrial purposes:

1. Magnesium Sulfate ($MgSO_4$) rejection of > 90 %.

2. Permeation flux of 20 gallon per square feet per day (gfd) or 8.73×10^{-5} $m^3/m^2.s$.

The reverse osmosis performance of the composite membranes is investigated by using different numbers of coating layers and various coating solution concentrations for membrane preparation. The effect of pore size and pore size distribution of the membranes to the separation and the permeation flux are also studied using log-normal probability plot and sieving curve correlation approaches.

CHAPTER TWO

THEORY AND METHODOLOGY

2.1. The fundamental of RO process

Reverse osmosis is based on the chemistry at interfaces of which the Gibbs adsorption equation, given in the form:

$$\Gamma = -\frac{1}{RT}\left(\frac{\partial \gamma}{\partial \ln a}\right)_{T,A} \qquad (1)$$

is just one expression. This equation indicates that surface forces can induce negative or positive adsorption of solute at interfaces, which in turn introduce steep concentration gradients at interfaces. The interfacial concentration gradient in effect gives rise to preferential sorption of one of the components of a solution at the interface. The preferential sorption is dependent upon the physicochemical interaction forces occurring at the interface. This concept is the fundamental basis of reverse osmosis separation and is expressed in terms of the preferential sorption-capillary flow mechanism involving an appropriate porous membrane.

2.2. The preferential sorption-capillary flow mechanism

From the point of view of the preferential sorption-capillary flow mechanism, any space between two unbounded material entities in the membrane matrix, through which space mass transport can take place during RO operating conditions, is a pore whose equivalent diameter can be expressed by any distance greater than zero, however small it is.

According to the mechanism, RO separation is governed by equilibrium effect and kinetic effect. The equilibrium effect is concerned with the preferential sorption in the area of the membrane surface and is governed by repulsive and/or attractive potential gradients in the vicinity. The kinetic effect is concerned with the mobility of solute and solvent through the membrane pores and is governed by the equilibrium effect and the steric effects associated with the structure and size of molecules relative to those of the pores on the membrane surface. Consequently, both the chemical nature of the membrane surface in contact with the solution and the existence of pores of appropriate size and number on the area of the membrane at the interface constitute the essential requirements for the success of a RO process.

Suppose the surface forces govern details of preferential sorption at membrane-solution interfaces and the transport of solute and solvent through membrane pores in reverse osmosis. If this is so, then any change in either the chemical nature of solute, that of solvent, that of the surface of the membrane material or the porous structure of the membrane surface changes membrane performance.

2.3. Surface Force-Pore Flow Model for RO

The surface force-pore flow model is a quantitative expression of the preferential sorption-capillary flow mechanism. In this model, the pores on the membrane surface are assumed equivalent to circular cylindrical pores, with or without a pore size distribution, and the solute-membrane material interactions relative to solvent (water) are expressed in terms of electrostatic or Lennard-Jones-type surface potential functions (Φ). The potential function representing electrostatic repulsion of ions at the interface due to relatively long-range coulombic forces is expressed as :

$$\Phi = \frac{\tilde{A}}{\underline{d}} \tag{2}$$

The Lennard-Jones-type potential function for nonionic solutes, which represents the sum of the relatively short-range van der Waals attractive force and the even shorter-range repulsive force due to overlap of electron clouds at the interface respectively, is expressed as:

$$\Phi = -\frac{\tilde{B}}{\underline{d}^3} + \frac{\tilde{C}}{\underline{d}^{12}} \tag{3}$$

$$\Phi \begin{cases} \text{very large, when} \quad \underline{d} \le \tilde{D} \\ \dfrac{\tilde{B}}{\underline{d}^3} \text{ , when} \quad \underline{d} \le \tilde{D} \end{cases}$$

and the friction function Ψ representing the friction force against the movement of solute, under the influence of the above surface forces, through the membrane pore is expressed as:

$$\Psi = \frac{\tilde{E}}{\underline{d}} \tag{4}$$

where $\tilde{A}, \tilde{B}, \tilde{C}, and \tilde{E}$ are the respective force constants characteristic of the interface, $\underline{d}$ is the distance between the membrane surface or pore wall and the solute molecule, and $\tilde{D}$ is the value of $\underline{d}$ at which Φ becomes very large. The friction function Ψ can also be expressed in different functional forms. Assigning appropriate values for the above quantities, one can obtain the potential functions for the membrane material-solution systems discussed above.

The transport of solute and solvent through the membrane pores is governed by such surface forces together with the friction forces and solution velocity profiles within the pores. Based on the above model, appropriate transport equations can be derived for an individual cylindrical pore of radius R and effective pore length δ. The derivations can then be extended to the multi-pore system of the actual membrane involving one or more equivalent average pore radius $\underline{R}$ and its standard deviation, σ, representing the pore size distribution. The foregoing analysis results in general expressions for solute separation and fluid flux which are valid whether the solute is negatively or positively adsorbed at the membrane-solution interface. Using the cylindrical coordinate system shown in Figure 7, the solute concentration and the velocity profile of the solution inside the membrane pore can be analyzed in differential segments as a function of (r,z) covering the entire pore region, under the steady state operating conditions of the process. The detailed derivations can be found in the literature (Zhou et al., 1991).

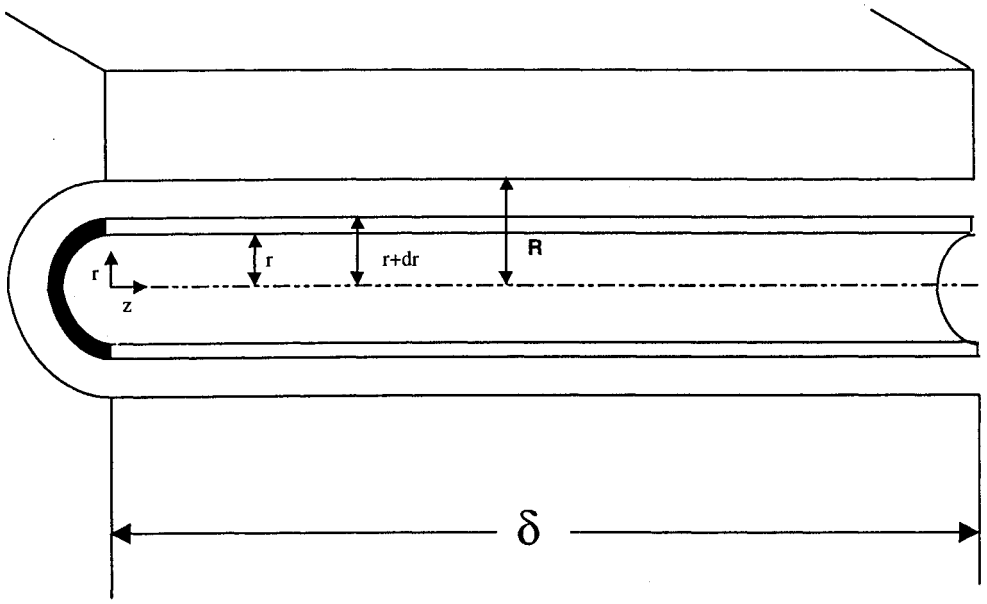

Figure 7. Cylindrical Coordinates in a Membrane Pore (Sourirajan and Matsuura, 1985)

2.4. Necessary refinement to the definitions of pore radius

In the foregoing discussions, the quantities R, $\underline{R}$, and σ represent pore radius, mean pore radius, and standard deviation in R, respectively. When we go from macroscopic to microscopic considerations, refinement with respect to R has to be made.

When the radius of water molecule (D_W) is significant compared to the radius of the membrane pore (R_b), which is the case with respect to RO/UF membranes, a distinction has to be made between the radius of the channel available for fluid flow and the actual size of the membrane pore.

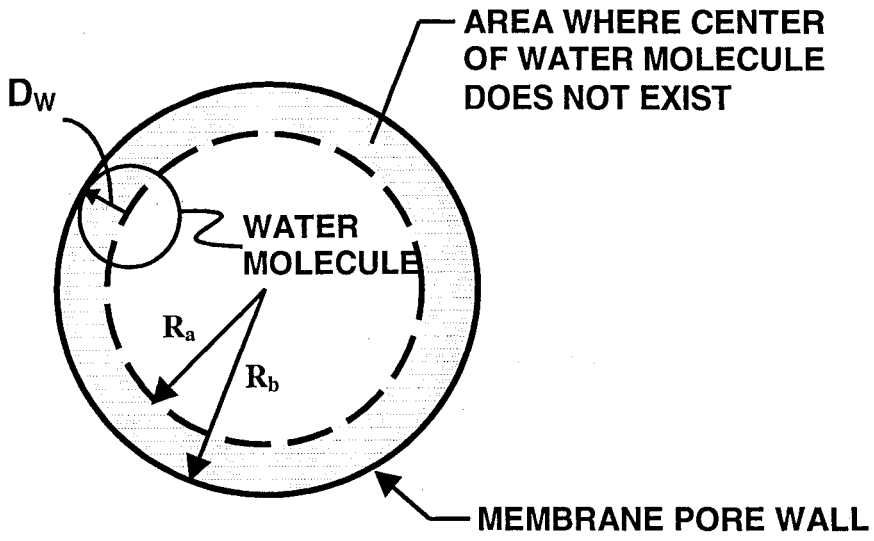

Figure 8. Position of Water Molecule in a Membrane Pore

Referring to Figure 8, let:

D_W = radius of water molecule

R_b = radius of membrane pore

$R_a = R_b - D_W$ = effective radius of membrane pore available for fluid flow.

For purpose of analysis, a molecule is considered to be spherical in shape and its location is defined as the location of its center. It means that the area where the center of the molecule cannot exist, the molecule as an entity does not exist. Hence there is no solution in the area.

2.5. Theory in Pore Size and Pore Size Distribution

While surface force-pore flow model gives a rigorous description of transport through the membrane pore, the acquisition of all required parameters is difficult. A sieving model is used, instead, as a simplified version of the pore model. In this model, it is assumed that molecules with sizes smaller than the pore radius go through the pore and those with larger sizes do not go through. Thus, the pore size and the pore size distribution on a membrane surface can be obtained from separation data of solutes of known sizes.

One of such attempts to obtain the pore size and the pore size distribution was made by Michaels (1980) using sieving coefficients, θ, for solutes of different Einstein Stoke Radius (ESR), given as "a", on the assumption that the pore size distribution follows the log-normal distribution. On such assumptions, namely the sieving model and the log-normal distribution, the following equations were derived:

$$\theta = 1 - erf(\tau) \tag{5}$$

where :

$$\tau = \frac{\log(\frac{a}{\underline{a}})}{\log \sigma_a} \tag{6}$$

$\underline{a}$ is the ESR of the "mean" macromolecule and σ_a is the geometric standard deviation about the mean ESR. In equation (5), erf means error function.

θ is directly related to experimental solute separation, f :

$$\theta = 1 - f \tag{7}$$

A linear relationship between θ and a (or f and a) is expected on log-normal probability plot according to equation (5) and (6), if the above assumptions are valid. $\underline{a}$ is obtained on the plot as an ESR corresponding to $\theta = 0.5$ (f = 50%). σ_a can be determined from the ratio of a at $\theta = 0.159$ (f = 84.1%) and a at $\theta = 0.5$ (Ishiguro et al., 1996; Michaels, 1980). For simplicity, f vs. a is plotted, instead of θ vs. a, on the log-normal probability plot.

From the slope of the log-normal probability plot, one can directly relate to the pore size distribution of the membrane. When the slope is steep, the ratio of a at f = 84.1% and a at f = 50% is small, therefore σ_a is small (the pore size distribution is narrow). When the slope is not steep, the ratio is large, therefore σ_a is large (wide pore size distribution).

2.6. Molecular Weight Cut-off

Molecular weight cut-off (MWCO) is a solute's molecular weight for which a membrane should achieve 90% separation. It is determined from the solute separation curve, where the membrane is subjected to a series of RO experiments using solutes with different molecular weights in feed solutions. In this experiment, the solute used to determine the MWCO of the membranes was polyethyleneglycol (PEG).

PEG separations for the membrane were plotted against their molecular weights, creating a PEG separation curve. Drawing a horizontal line from the y-axis at 90% separation to the curve yields a molecular weight that corresponds to the separation. This molecular weight is referred to as the molecular weight cut-off (MWCO). In the case where the 90%

separation fell between two experimental points in the curve, then a linear interpolation is used to determine the corresponding molecular weight. For the case where the PEG separation curve constructed does not reach a 90% separation, a linear extrapolation is used.

2.7. Solute Separation

The transport of solute across a membrane is commonly expressed as solute passage or solute separation. Solute passage is the percentage of the solute in the feed that passes through the membrane into the permeate, whereas solute separation is the percentage of the solute in the feed that does not pass through the membrane.

Solute separation is calculated as follows :

$$f = (C_f - C_p) / C_f \times 100 \qquad (8)$$

where : f = % solute separation
C_p = solute concentration in product stream
C_f = solute concentration in feed stream

CHAPTER THREE

EXPERIMENTAL

A RO test cell is made of stainless steel 310 and consists of two detachable parts. The upper part is a high-pressure chamber. A membrane is mounted on a stainless steel porous plate embedded in the lower part of the cell such that the active surface layer of the asymmetric membrane faces the feed solution under high pressure. A wet Whatman filter paper is placed between the membrane and the porous plate to protect the membrane from abrasion. Figure 9 shows the diagram of a reverse osmosis test cell.

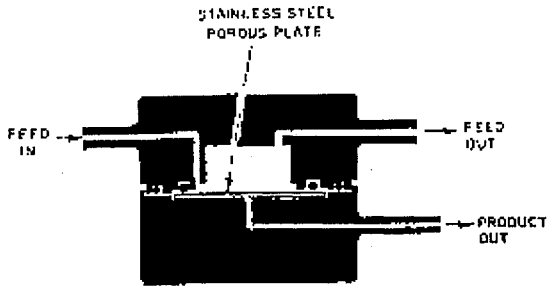

Figure 9. A Reverse Osmosis Test Cell

3.1. Experimental Setup

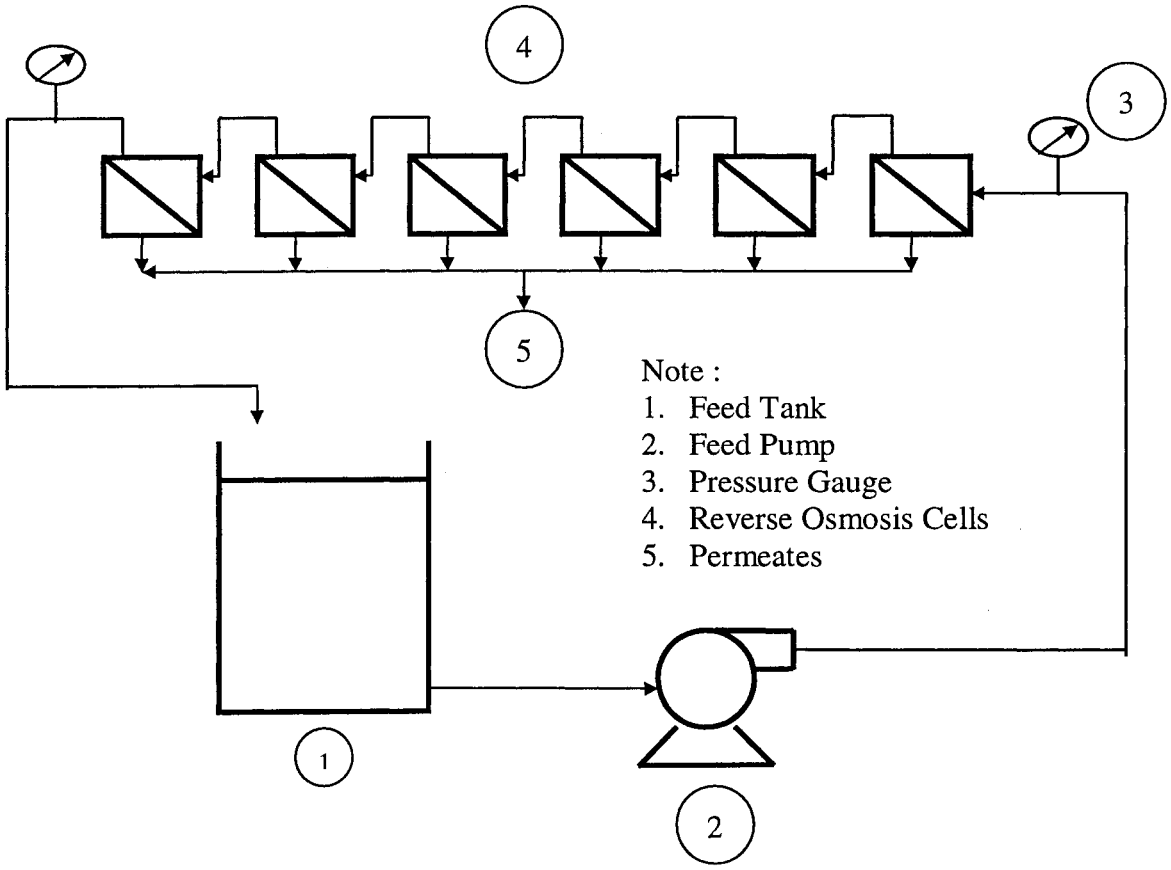

Figure 10. Experimental Setup of Reverse Osmosis System

The reverse osmosis experiments were conducted using six high-pressure permeation cells with effective membrane areas of 10.2 cm^2. The cells were connected in series. The feed came from the feed tank and was transported to the cells via a feed pump. The feed was then returned from the last cell to the feed tank. Two pressure gauges were located at both ends of the RO cells setup to check the pressure drop across the cells. Permeates from each cell were collected and treated individually to check their permeation rates and electrolyte

concentrations. The electrolyte concentrations of permeates or of the feed were measured using a conductivity meter (refer to Figure 10).

3.2. Material

3.2.1. Substrate membranes

The following commercial ultrafiltration membranes were used as microporous substrate membranes to prepare thin film composite membranes. AP-10 membrane was generously supplied by Osmonics, Inc. and is based on polyvinylidenefluoride. HW-18 membrane, also supplied by Osmonics, Inc., is made from polyethersulfone on polyester fibres as backing material employing the phase inversion technique (Hamza et al., 1995). E-500 membrane is based on polyethersulfone and was supplied by Desal System, Inc. Both HW-18 and E-500 membranes have maximum operating conditions of 100°C and pH range of 1-13. The maximum operating pressure for HW-18 is 14 x 10^5 N/m^2, whereas for E-500 is in the range of 2-6 x10^5 N/m^2 (Ho and Sirkar, 1992).

3.2.2. Coating solution for TFC membrane

Poly (2,6-dimethyl-1,4-phenyleneoxide), PPO, was supplied by General Electric Co., St. Louis, Missouri. As mentioned earlier, Tg of PPO is 212°C (Petersen, 1993) and the initial decomposition temperature for this polymer is 470°C at a heating rate of 10°C/min (Fu et al., 1994). The intrinsic viscosity [η] in chloroform for the PPO polymer used in the project was 1.79 dL/g at 25°C. The molecular weight of PPO polymer was approximately 50,000 -

60,000. The viscosity value was chosen because it will give the necessary strength for the polymer to be placed as an ultrathin layer on the supporting membrane. The greater the intrinsic viscosity for a polymer is, the stronger it is mechanically (more durable). However, increasing the intrinsic viscosity beyond this point will also mean introducing stiffness that is not desirable for the ultrathin layer because it will create fragility due to its very small thickness.

For sulfonation of PPO, the reagent used was chlorosulfonic acid, having a density of 1.75 g/cm^3 at 20°C and a minimum assay of 97%, obtained from BDH Corporation, Toronto, Ontario. Solvent used for sulfonated PPO (SPPO) was methanol and chloroform. Methanol (CH_3OH), supplied by BDH, Toronto, Ontario, had a density of 0.79 g/cm^3 and a minimum assay of 99.8%. Chloroform ($CHCl_3$), stabilized with a nonpolar hydrocarbon, had a density of 1.49 g/cm^3 and a minimum assay of 99.9%. Chloroform supplied by OmniSolve. Solvent was of reagent grade and used without further purification.

3.3. Preparation of polymer for coating

3.3.1. Sulfonation of PPO

Poly (2,6-dimethyl-1,4-phenyleneoxide) or known as PPO was used without any further treatment. A 10wt% PPO solution was prepared by dissolving the polymer in chloroform at room temperature. Chlorosulfonic acid was introduced according to the method described in Plummer et al. (1970), i.e. via a dropping funnel over a period of 20 min while the solution was stirred vigorously and allowed to react for an additional 20 min at room

temperature. As sulfonation progressed, sulfonated poly (2,6-dimethyl-1,4-phenylene oxide), SPPO, precipitated from the solution since SPPO is insoluble in chloroform. The precipitate was dissolved in methanol, filtered, and washed thoroughly with distilled water, until the wash water showed a pH value of 4 (Chowdhury et al., 1994). It was then dried exhaustively at room temperature under vacuum for 2 days.

3.3.2. Determining the IEC value of sulfonated PPO

One of the methods to determine the IEC value of a SPPO in hydrogen form, abbreviated as SPPO-H, is by using a conventional acid-base titration method. A weighed amount (0.5670 g) of dry polymer was placed in a glass beaker filled with 25 ml of 0.1 N sodium hydroxide. Phenolphthalein was added as a pH indicator. Then 0.1 N hydrochloric acid was added dropwise to the beaker. The volume used for the solution to be neutral was recorded. The polymer in acid form exchanges with sodium, liberating H^+ ions which consume a stoichiometric amount of hydroxide. From there, the IEC value can be calculated as follow:

$$IEC = \frac{v \times N_{NaOH}}{w} \qquad (9)$$

where : IEC = Ion exchange capactity (meq/g dry polymer)

v = volume of NaOH used in titration (mL).

N_{NaOH} = Normality of NaOH solution used.

w = weight of SPPO polymer.

The ion-exchange capacity (IEC) of the SPPO polymer prepared by the method described in section 3.3.1 was 1.87 meq/g of dry polymer. The calculation will be described in the appendix.

3.3.3. Changing acid form of SPPO to a salt form

Conversion of an acid form of SPPO to a stable salt form can generally be accomplished by contacting the solid acid form of SPPO with an aqueous salt solution, preferably a base solution such as sodium or potassium hydroxide solution (Fu et al., 1994). The same procedure as used in determining the IEC value was also used to convert the SPPO polymer to a salt form. Excess sodium hydroxide solution was used for converting SPPO from acid free form (SPPO-H) to salt form (SPPO-Na). After equilibrating the polymer with the sodium hydroxide solution, the solid is rinsed with distilled water to remove excess electrolytes and dried.

3.4. Thin film composite membrane preparation

Coating solution was made by dissolving 0.4 g of SPPO in free acid form in 40 g of methanol to give 1.0wt% solution of SPPO-H and by dissolving 0.2, 0.3 and 0.4 g of SPPO in sodium form in 40 g of methanol to give 0.5, 0.75 and 1.0wt% solution of SPPO-Na. Methanol was chosen as solvent because it is polar, inert with SPPO and has a low boiling point. Moreover, it was observed to not react with substrate membrane.

One ml of coating solution was spread over the substrate membrane surface that was secured on top of a glass jar. Excess of coating solution was drained in a circular motion. The coated membrane was let to dry overnight under ambient temperature before use.

3.5. Heat treatment of composite membranes

For membranes subjected to post treatment, the following treatments were employed on the newly coated membranes before the membranes were compacted and tested.

3.5.1. Annealing

Membranes were placed in an oven without forced air circulation at a preset temperature (in this case 60°C and 100°C) and for a preset heating period (5 hours and 0.5 hours) directly after coating was employed.

3.5.2. Heat treatment under water

Membranes were placed in a beaker filled with water at 84°C after being coated and dried overnight. The period of treatment was varied from 2.5 hours to 6 hours. The membranes were then immediately placed in the cell for compaction and testing.

3.6. Pore Size Determination

Pore size of a membrane is very crucial since it determines the performance of the membrane in both selectivity and permeation flux. To characterize the membrane, feed

solution containing polymeric solutes which belong to a homologous series and are of different molecular weights are separated by a membrane. Solutes used for this purpose are usually polyethylene glycol (PEG), polyethylene oxide (PEO) and dextran. The molecular weight of the solute corresponding to 90% separation is termed as the Molecular Weight Cut Off (MWCO) of a membrane and used as an indicator of the pore size.

A method of determining the pore size and the pore size distribution of a membrane was studied by Ishiguro et al. (1996) based on sieving curves approach described by Michaels (1980). More information on how the method is employed can be referred to in the theoretical part of this thesis.

3.7. Membrane testing

First, membranes were compacted by distilled water under 400 psig for approximately 40 hours. The rate of permeation was recorded at an interval of 2 hours. Membranes were then tested at an operating pressure of 150 psig (1.02 MPa) and room temperature (25°C) with different feed solutions. The feed solution was circulated through the feed chamber of the permeation cells and the flow rate was observed to be in the range of 1.195 m^3/day. For each experiment, pure water permeation rate (PWP) and permeate flux (PF) in the presence of the solute in the feed and solute separation were determined. PWP was calculated based on the amount of water permeating through the membrane, when the feed was pure water, in a preset time. Depending on the permeate flux (PF), an arbitrary time of 3 - 5 minute was used. PF was calculated using the same basis as PWP, only this time the feed contained a

solute. The PWP and the permeate flux were then converted to that at 25°C using density and viscosity data of water. The conversion table for the permeation rate with regard to the change of temperature was prepared in the Appendix C. For each feed solution used in the experiment, three runs was carried out. The results were then averaged and presented in either a table form or a graphic form.

3.7.1. RO test with electrolyte solution

$MgSO_4$ solution with a concentration of 1500 ppm was used as feed to study the electrolyte separation characteristic of the membranes. Determination of the electrolyte content both in the feed and in permeates during the runs was carried out using CDM-80 conductivity meter, manufactured by Radiometer A/S, Copenhagen. A calibration curve was made to relate the conductance to the electrolyte concentration. Electrolyte separation was calculated using equation (8) in the theoretical section.

3.7.2. RO test with polyethyleneglycol solutions.

Polyethyleneglycol (PEG) solutes with different molecular weights (from 200 - 9000) were introduced to the feed. The concentration of PEG in the feed was approximately 200 ppm. The permeation rate was recorded and the concentration of PEG was determined using Beckman 915B Total Organic Carbon Analyzer. PEG separation was also calculated using equation (8) in the theoretical section. PEG separation curve was constructed based on the PEG separation data and MWCO of membranes was determined.

CHAPTER FOUR

Results and Discussion

4.1. Substrate membrane

Table 1 shows the $MgSO_4$ separations for the substrate membranes. Membrane AP-10 was observed to have the lowest $MgSO_4$ separation (16%) compared to the other substrate membranes. However, it had the highest permeate flux (PF) of $3.00x10^{-4}$ $m^3/m^2.s$. On the other hand, membrane HW-18 had the highest $MgSO_4$ separation (27%). However, its permeate flux was the lowest among all ($1.17x10^{-4}$ $m^3/m^2.s$). Membrane E-500 was observed to have $MgSO_4$ separation closes to that of HW-18 (23%) with permeate flux nearly 1.5 times that of HW-18. $MgSO_4$ concentration in the feed solution was kept at 1500 ppm for all the experiments.

Table 1. RO Performance of Substrate Membranes

Substrate Membrane	PWP * ($x10^{-5}m^3/m^2.s$)	PF ($x10^{-5}m^3/m^2.s$)	Separation (%) $MgSO_4$,1500ppm
AP-10	38.3	30.0	16.4±1.5
HW-18	11.7	11.6	27.4±1.0
DESAL E-500	16.8	16.4	23.0±0.8

* PWP = pure water permeation flux

Molecular-weight-cut-off (MWCO), as described in the theoretical part, of membranes AP-10, HW-18 and E-500 were determined from the separation data of polyethylene glycol (PEG) of different molecular weights. MWCO were determined from Figure 11 and were found to be 8000, 2900 and 3900 for AP-10, HW-18 and E-500, respectively. The error bars in Figure 11 represents standard deviations of each point in the separation data.

During the PEG separation experiments, permeate flux (PF) for the membranes were also measured (refer to Figure 11). The permeate flux to be mentioned represents the average flux of all separation experiments with different molecular weights for each membrane. Membrane HW-18 was found to have an average permeate flux of 11.0×10^{-5} $m^3/m^2.s$, while membrane E-500 and membrane AP-10 had an average flux of 18.0×10^{-5} $m^3/m^2.s$ and 37.0×10^{-5} $m^3/m^2.s$, respectively. Except for membrane E-500, the permeate fluxes of PEG separation data were relatively constant. Therefore, it can be considered that no fouling has occurred in those two membranes. The calculation of the pore size would then represent the actual pore size of the membrane without any effect of fouling. In the case of PF of membrane E-500, the line showed a slight decrease during the experiment. It may be that in the pre-test, the membrane had not undergone compaction and thus its PF was still stabilizing. It may also be due to some error during the experiment itself.

PEG separation curve for AP-10 showed a very small incremental change in % separation of PEG with PEG molecular weight increase. This may indicate that this membrane had a very wide range of pore size distribution. In another word, the pore sizes in this membrane were least uniform.

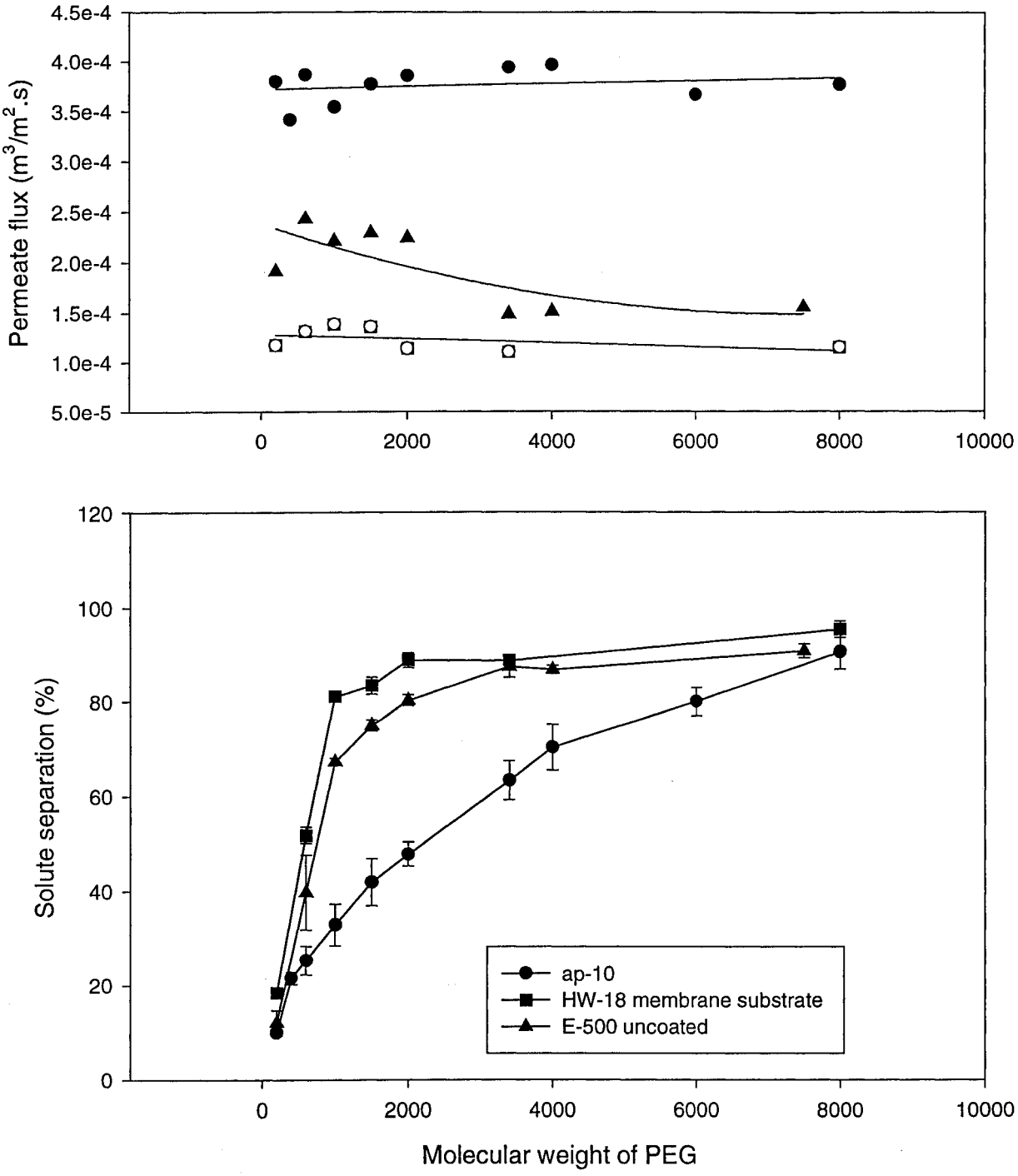

Figure 11. PEG Separation and Permeate Flux versus Molecular Weight for Substrate Membranes

A method for determining the pore size and the pore size distribution in a membrane used by Ishiguro et al. (1996) was employed. Instead of using the sieving coefficient, θ, which is equal to 1 – separation, (1-f), the separations for the PEG of different molecular weights, f, were plotted against the Einstein-Stokes radius (ESR), or referred to as "a", in a log-normal probability plot (refer to Figure 12). The corresponding ESR for different molecular weight of PEG solute can be seen in Table 2.

Table 2. Einstein-Stokes Radius for Different Molecular Weight of PEG Macromolecule (Ishiguro et al., 1996)

Molecular Weight (Dalton)	Einstein-Stokes Radius (x 10^{10}, m)
200	3.86
300	4.56
400	5.16
600	6.27
1000	7.89
1500	9.85
2000	11.43
4000	15.34
9000	28.9
20000	31.0

From equation (5) and (6) in the theory section, it was expected that plotting θ vs. a (or f vs. a) on a log-normal plot will result in a straight line.

According to the theory, the geometric standard deviation in the pore size, σ_a, can be determined from the ratio of a at $\theta = 0.159$ (f = 84.1%) and a at $\theta = 0.5$ (f = 50%). The ESR of the mean macromolecule, $\underline{a}$, is determined by the ESR which corresponds to a separation of 50%. The standard deviation, σ_a, indicates the uniformity of the pore size distribution,

while a indicates the mean pore size. The steeper the slope of the plot is, the smaller is σ_a and thus, the narrower is the pore size distribution of the membrane.

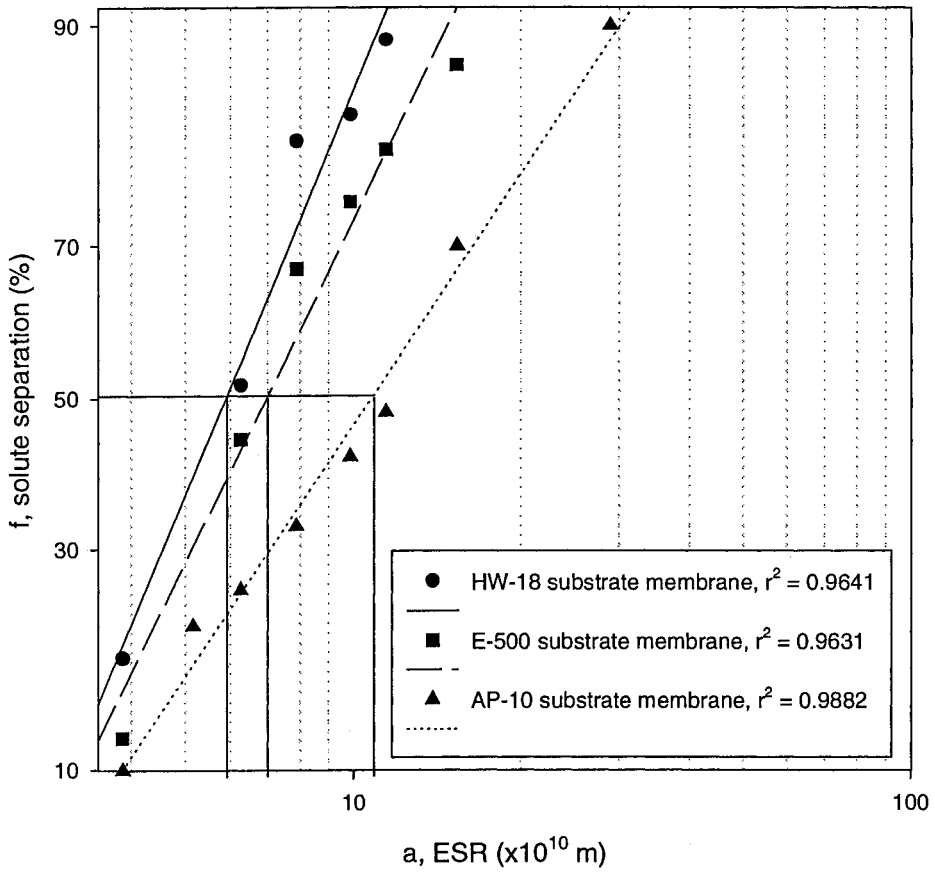

Figure 12. Pore Size Distribution for Substrate Membranes

Looking at Figure 12, HW-18 shows the largest slope, whereas AP-10 shows the smallest slope. This indicates that pore size distribution of AP-10 is broader than E-500 and HW-18. The mean pore size for AP-10 was the largest (10.5×10^{-10} m) compared to E-500 and HW-18 (6.9×10^{-10} m and 5.8×10^{-10} m, respectively). This may explain why the separation was lower and permeate flux was higher for AP-10 than other membranes.

Thin film composite membranes (TFC) were made by coating 1 layer of 1.0wt% SPPO-H solution on all the three membranes described so far. Composite membranes made were then subjected to reverse osmosis experiments. It was observed that the $MgSO_4$ separation for the coated AP-10 was still the lowest (38%) compared to those of coated HW-18 (70%) and coated E-500 (59%) although its permeate flux (PF) was higher than the others (Table 3). Nevertheless, the results indicated an improvement in the separation from the previous experiment (Table 2), using only substrate membranes without coating.

Table 3. RO Performance of TFC Membranes Coated by 1 Layer of 1.0wt% SPPO-H

Membrane Type	PWP ($x10^{-5}m^3/m^2.s$)	PF ($x10^{-5}m^3/m^2.s$)	Separation,% $MgSO_4$,1500ppm
coated AP-10	13.8	14.1	38.0 $\pm$ 1.1
coated HW-18	5.5	6.8	69.6$\pm$0.8
coated E-500	9.5	10.5	59.1$\pm$0.9

PEG separation experiments were also carried out for the three composite membranes. Figure 13 shows that MWCO of coated AP-10 was quite high (around 2000), whereas those of coated HW-18 and coated E-500 were around 900 and 1100.

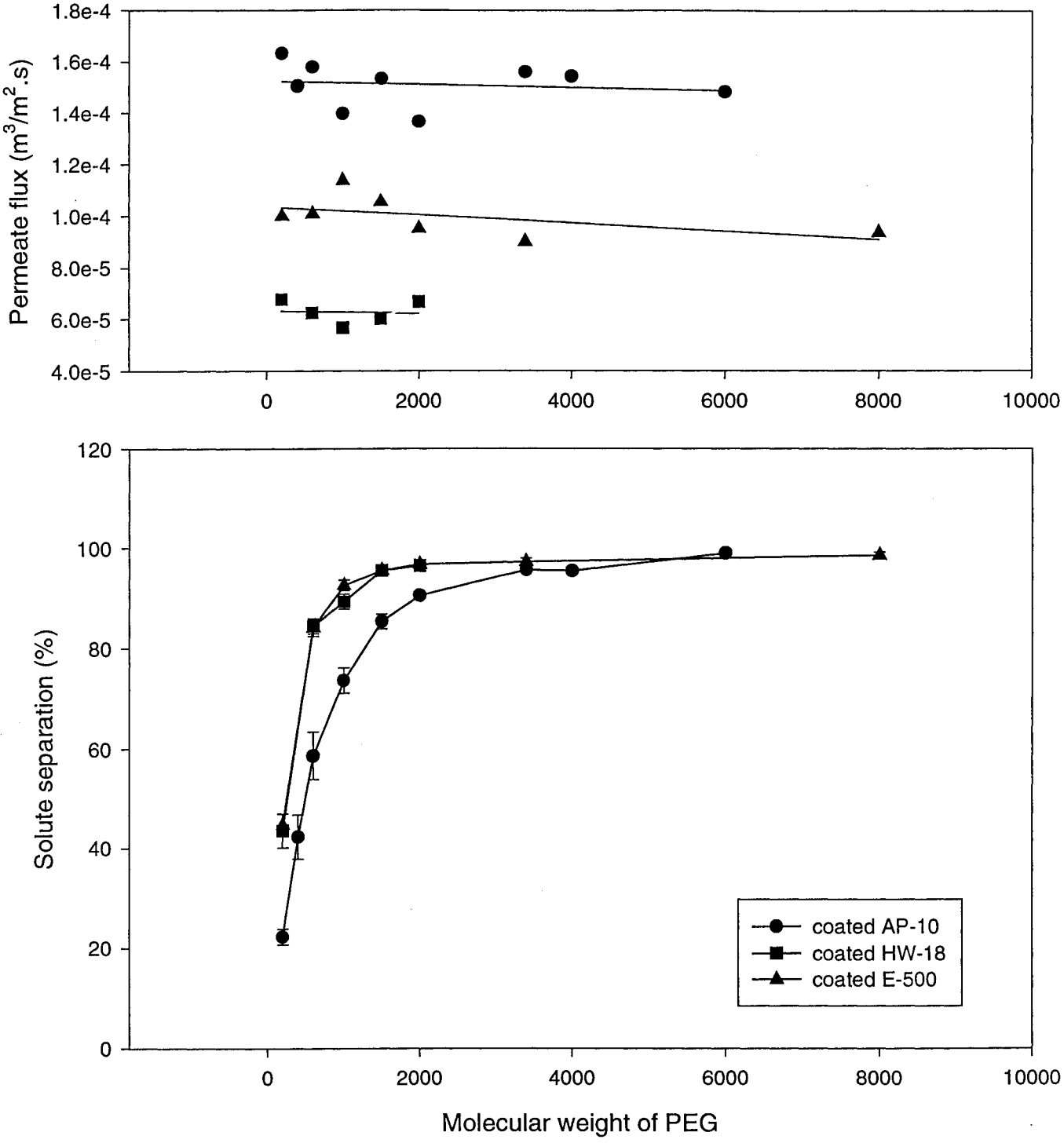

Figure 13. PEG Separation and Permeate Flux for TFC Membranes Coated with 1 Layer of 1.0wt% SPPO-H Solution

Looking at the permeate flux for the membranes, coated AP-10 showed the highest permeate flux ($15.0x10^{-5}$ $m^3/m^2.s$) whereas permeate flux of coated HW-18 was the lowest of all the TFC membranes ($7.0x10^{-5}$ $m^3/m^2.s$).

Analyzing the pore size distribution using the log-normal probability plot (Figure 14), it was found that the slopes for all the TFC membranes were similar, meaning that the geometric standard deviations for the TFC membranes were close to each other.

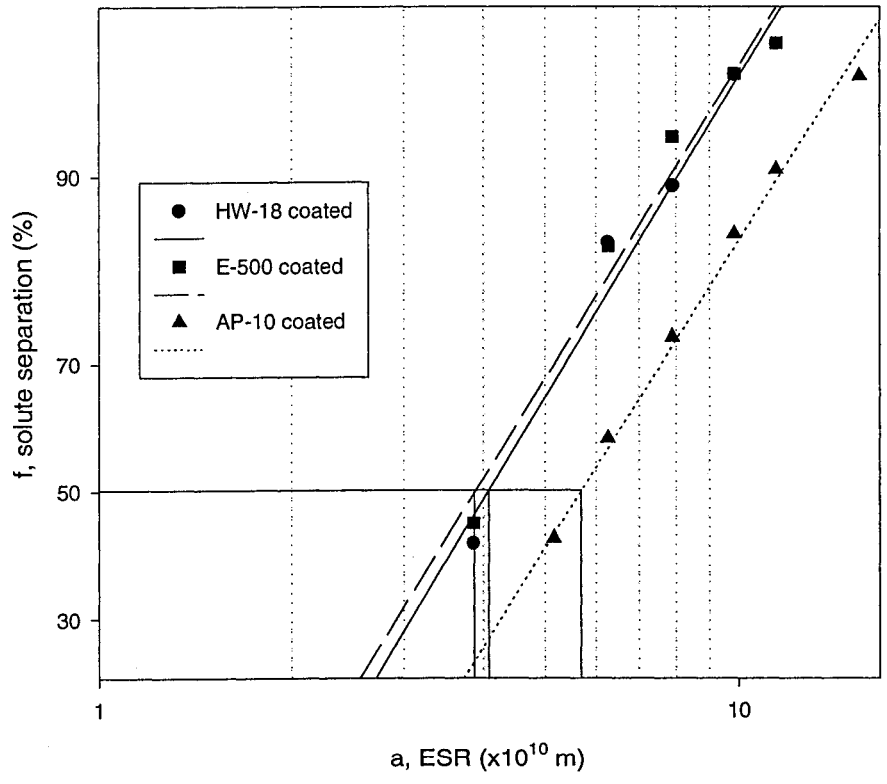

Figure 14. Pore Size and Pore Size Distribution of TFC Membranes

However, the mean pore size for the coated AP-10 was higher ($5.7x10^{-10}$ m) than coated HW-18 or E-500 ($3.8x10^{-10}$ m and $4.1x10^{-10}$ m, respectively). Thus, although the standard deviations for the three TFC membranes were similar, higher mean pore size (for AP-10) resulted in a lower separation of $MgSO_4$, as shown in Table 3. This left us with two choices for the selections of substrate membranes, i.e. HW-18 and E-500.

Based on the above experimental results, E-500 was chosen as the best candidate for the substrate membrane, since it has sufficiently uniform pore size (indicated by small σ_a, refer to Figure 12 and Figure 14) and a larger number of pores or a thinner top selective layer (indicated by high permeation rate, refer to Table 1 and Table 3) than HW-18 substrate membrane.

To preserve the chemical composition of the sulfonated PPO (SPPO), the polymer was then changed from its hydrogen form to sodium form. Thereafter the polymer is referred to as SPPO-Na.

4.2. Effect of number of coating layers on RO performance of TFC membrane

To observe the effect of the number of coating layers on electrolyte separation of composite membranes, the number of coating layers was varied from 1 to 3. In these experiments, substrate E-500 was chosen to be coated with 0.5wt% SPPO-Na solution. The results are shown in Table 4.

Table 4. Effect of Number of Coating Layers on RO Performance of TFC E-500 Membranes Coated by 0.5wt% SPPO-Na Solution

Solute and concentration	number of layers	PWP ($x10^{-5}m^3/m^2.s$)	PF ($x10^{-5}m^3/m^2.s$)	Separation %
$MgSO_4$ 1500 ppm	1	7.2	6.9	72.0 ± 3.4
	2	7.8	6.6	74.2 ± 0.9
	3	4.8	4.6	89.0 ± 4.6

Increasing the number of layers from 1 to 2 resulted in a marginal increase in the $MgSO_4$ separation and also in the permeation rate. After 3 coatings, the $MgSO_4$ separation was increased to 89%. However, the permeate flux of the membrane with 3 coating layers decreased to 4.6 $x10^{-5}m^3/m^2.s$ from 6.9 $x10^{-5}m^3/m^2.s$ with 1 layer of coating. Comparison of PEG separation curves for different number of coating layers is presented in Figure 15. MWCO for 1 layer and 3 layers of coating were observed to be close to 600, whereas MWCO for 2 layers of coating was around 1000. The decrease in the selectivity of 2 layers of coating may be attributed to the experimental error or to the substrate membrane defect.

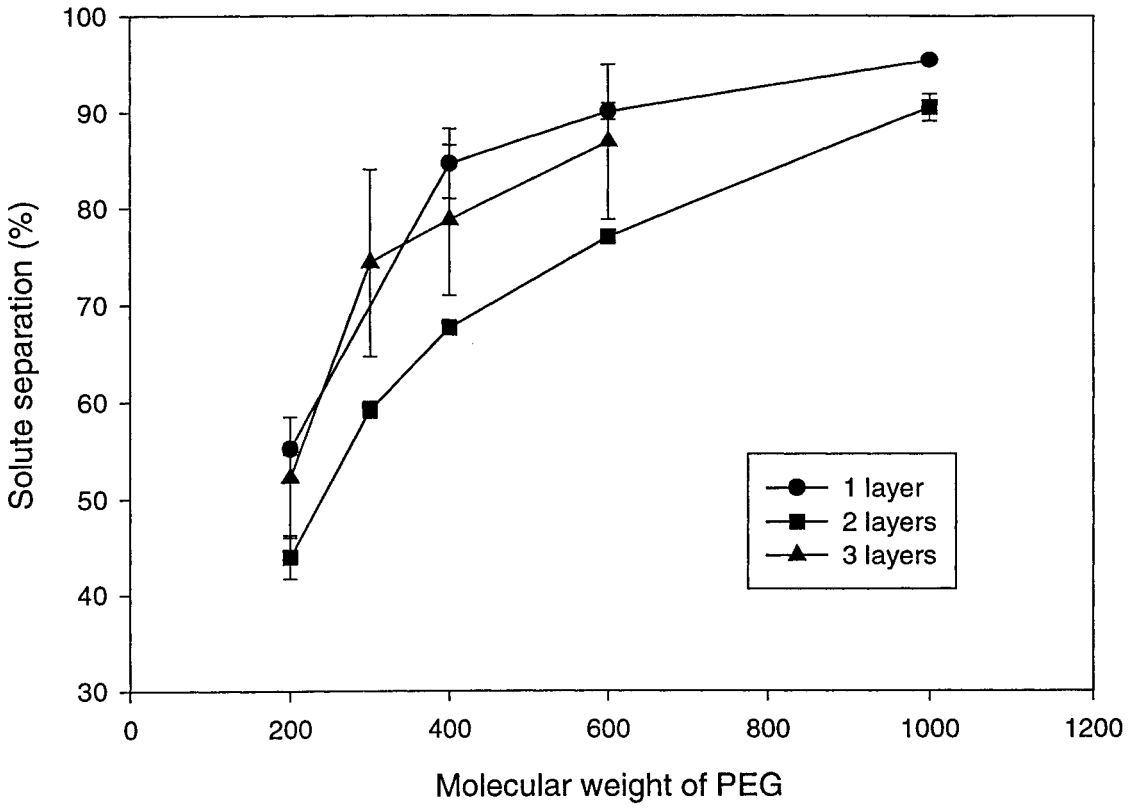

Figure 15. Effect of Number of Coating Layers on PEG Separations of E-500 Membranes Coated with 0.5wt% SPPO-Na Solutions

The log-normal probability plot of solute separation vs. ESR is given in Figure 16 for the membranes with different number of coatings. From the figure, the slope of 3 layers of coating was observed to be the largest followed by that of 1 layer as the second largest and that of 2 layers was the smallest in magnitude. This means that the pore size distribution of the membrane having 2 layers of coating was actually broader than those having 1 layer and 3 layers of coating. Also note that the mean pore size for 2 layers of coating (4.1×10^{-10} m) was higher than that of others (3.5×10^{-10} m and 3.7×10^{-10} m for 1 layer and 3 layer, respectively). It may be possible that in the production of the commercial membrane sheet

used as a substrate membrane in this work, there were some areas of non-uniform pore size distribution.

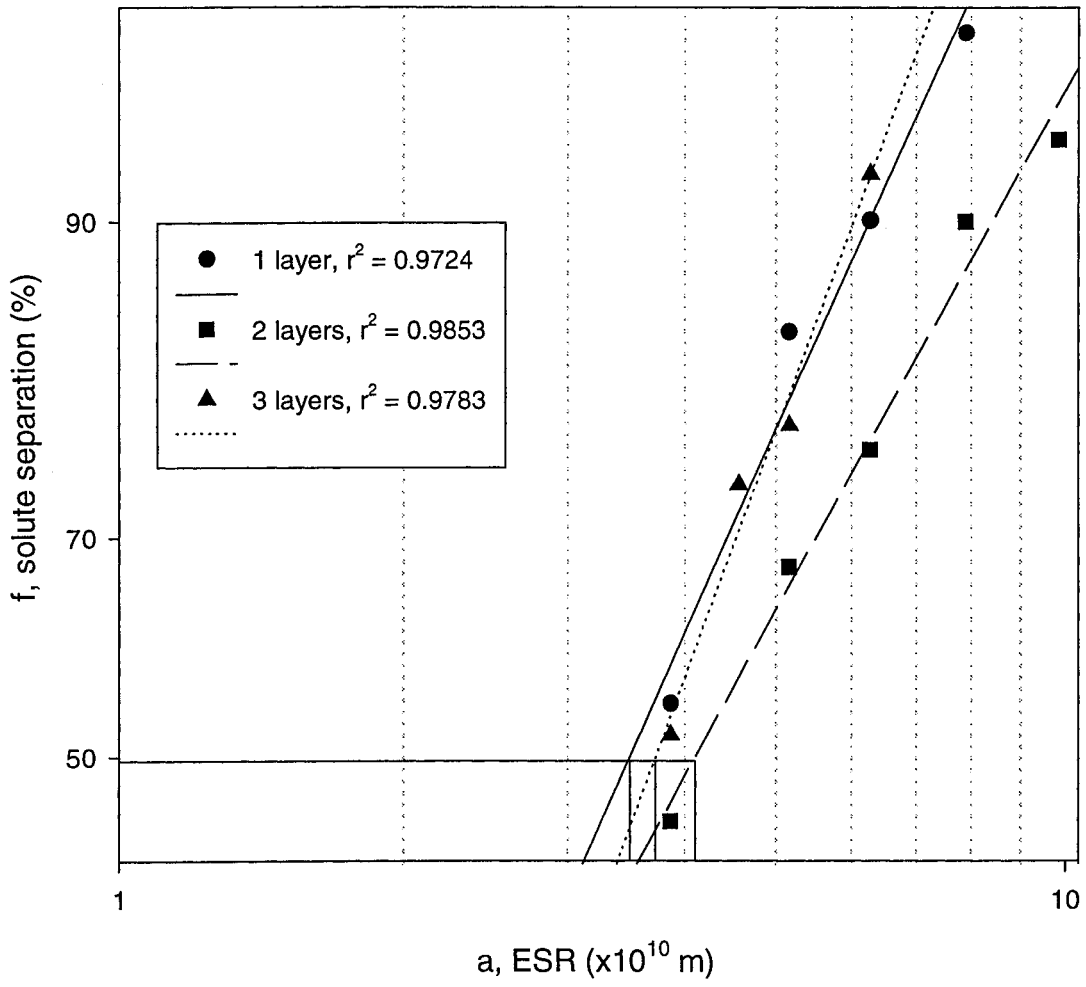

Figure 16. Effect of Number of Coating Layers on Pore Size and Pore Size Distribution (0.5wt% SPPO-Na on E-500 TFC Membranes)

The broad pore size distribution and the high mean pore size explain why the $MgSO_4$ separation did not increase significantly with increasing the number of layers coated on the substrate membrane from 1 to 2. Having a narrower pore size distribution compared to the membrane coated with 1 layer of SPPO-Na, the membrane coated with 3 layers of SPPO-

Na had a significantly higher $MgSO_4$ separation. However, the permeate flux with 3 layers of coating went down, maybe because of an increase in the skin layer thickness and/or may be because of the reduction in the mean pore size.

Since the project is aimed to attain a permeate flux higher than or equal to $8.7x10^{-5}$ $m^3/m^2.s$ at the given operating conditions, one layer of coating was considered sufficient for the purpose.

4.3. Effect of changing the coating solution concentrations on RO performance of TFC membranes

Composite membranes were prepared using coating solutions of different concentrations. RO experiments were carried out to see the effect of concentrations on membrane performance. One layer of coating of solutions with 0.5, 0.75 and 1.0wt% concentrations of SPPO-Na was applied on an E-500 substrate membrane.

Tables 5 shows the results of $MgSO_4$ separation and permeate flux for each coating solution concentration. The maximum separation of 93.5% was observed on a membrane with a coating concentration of 0.75wt% SPPO-Na solution. Surprisingly, the separation of $MgSO_4$ for 1.0wt% coating solution was found to be similar to that of 0.5wt% coating solution (around 72.0%) although the permeate flux of 1.0wt% coating solution was three times lower than that of 0.5wt% solution ($6.9\ x10^{-5}$ $m^3/m^2.s$ and $2.0\ x10^{-5}$ $m^3/m^2.s$ for

0.5wt% and 1.0wt%, respectively). Due to the low electrolyte separation, the membrane with 1.0wt% solution concentration was excluded from further experiments.

Table 5. Effect of Coating Solution Concentration on RO Performance of E-500

Feed (concentration)	Coating solution concentration (wt%)	PWP ($x10^{-5}m^3/m^2.s$)	PF ($x10^{-5}m^3/m^2.s$)	Separation %
$MgSO_4$ (1500ppm)	0.50	7.2	6.9	72.01±3.4
	0.75	4.4	4.6	93.51±3.0
	1.00	2.2	2.0	71.73±1.1

The effect of varying coating solution concentration on PEG separations of E-500 TFC membranes is shown in Figure 17. MWCO of the membranes with the coating solution concentration of 0.5wt% and 0.75wt% were observed to be around 600 and 500, respectively.

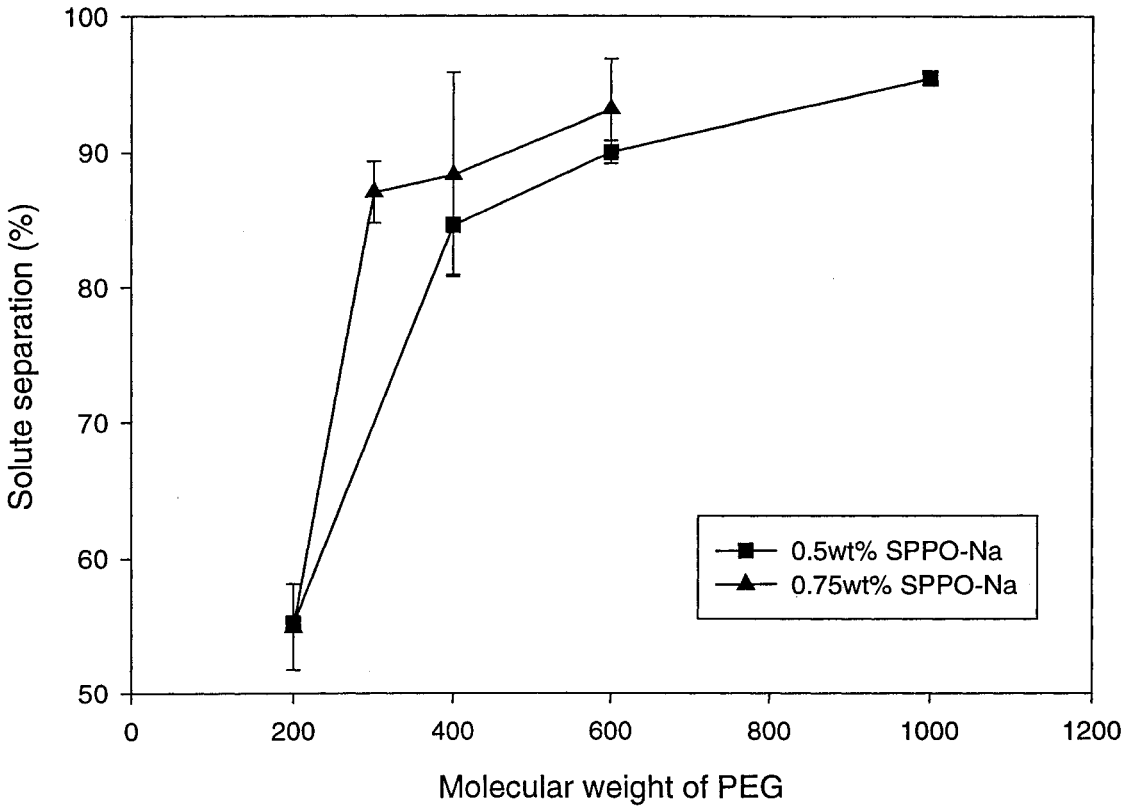

Figure 17. Effect of Coating Solution Concentration on PEG Separation of TFC Membranes

Figure 18 shows the log-normal probability plot of solute separation vs. ESR for the membranes coated with 0.5wt% and 0.75wt% solution concentration. As shown, the slope for 0.75wt% was steeper than that for 0.5wt% coating solution concentration. This shows that the membrane coated with 0.75wt% solution concentration had a narrower pore size distribution than that coated with 0.5wt% solution concentration. The mean pore size for 0.75wt% coating solution was also found to be slightly smaller (3.3×10^{-10} m) than that of 0.5wt% (3.5×10^{-10} m). As expected, this is what brought the high salt separation and the low permeate flux in 0.75wt%. Since the salt separation achieved for 0.75wt% coating solution concentration was closer to the goal of 90% $MgSO_4$ separation, it was concluded

that the optimum coating solution concentration was 0.75wt%, as far as the separation is concerned. However, permeate flux of this membrane was still lower than the target value.

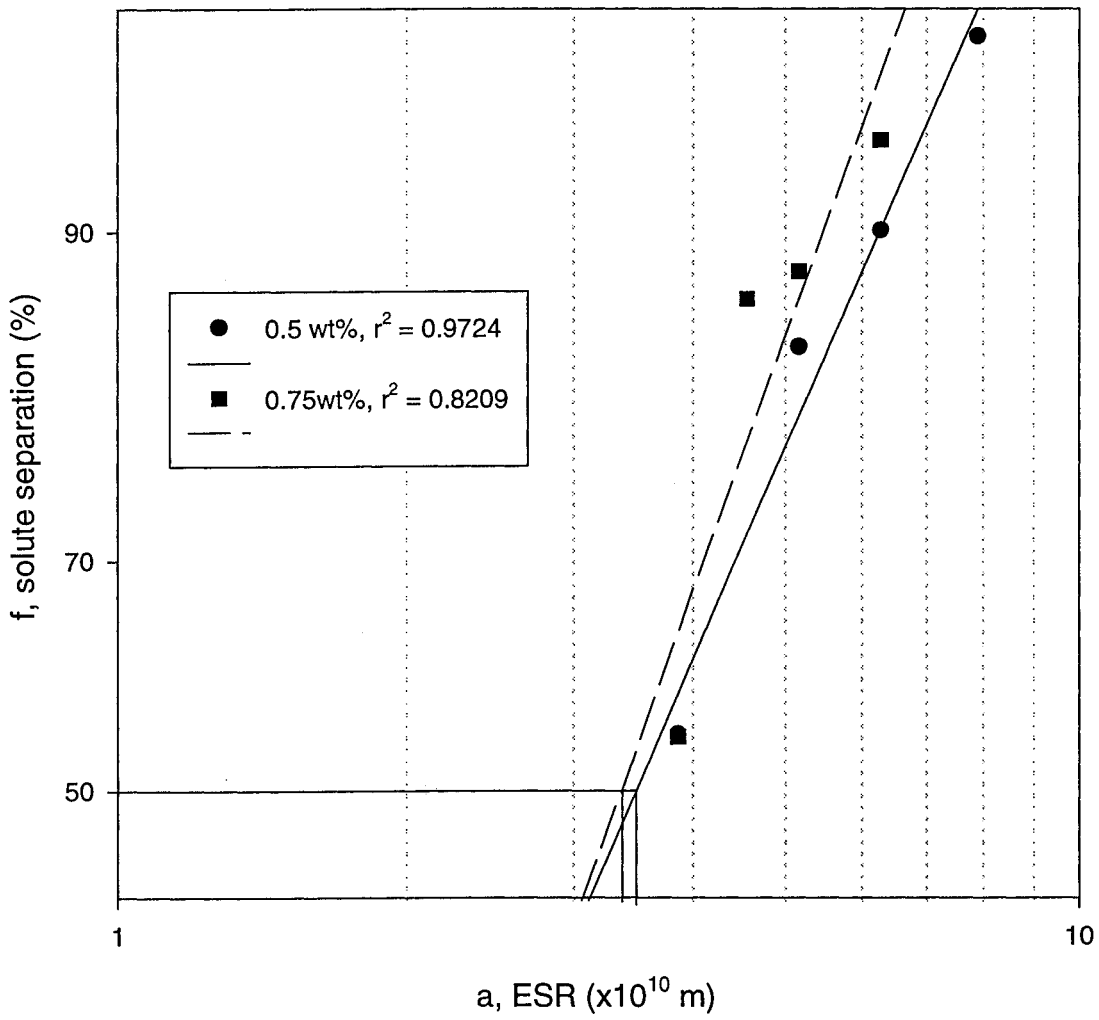

Figure 18. Effect of Coating Solution Concentration on Pore Size and Pore Size Distribution of TFC Membranes

4.4. Effect of heat treatment on RO performance of TFC membranes

4.4.1. Effect of annealing

To improve both the electrolyte separation and permeate flux, a heat treatment was considered. One method of heat treatment was annealing. The procedure of this treatment was described in the experimental part of this work.

It was expected that annealing decreases permeate flux while increases the electrolyte separation. Since it has higher permeate flux, the membrane coated with 1 layer of SPPO-Na with concentration of 0.5wt% was used instead of that with 0.75wt% coating solution concentration.

Table 6 shows that annealing at 60°C for 5 hours decreased the $MgSO_4$ separation from 72% (for membrane with no treatment) to 57%. Interestingly, permeate flux was almost doubled, from about $6.9x10^{-5}$ $m^3/m^2.s$ to $13.8x10^{-5}$ $m^3/m^2.s$. Annealing at 100°C for ½ hours increased the $MgSO_4$ separation from 72% (for no treatment) to 95%. However, permeation rate went down from $6.9x10^{-5}$ $m^3/m^2.s$ to $2.4x10^{-5}$ $m^3/m^2.s$.

It was conjectured that annealing at 60°C opened up the membrane pores. Thus, permeate flux went up and the solute separation went down. Annealing at 100°C, although the duration for the treatment was reduced, decreased the membrane pore sizes compared to membrane annealed at 60°C, thus, giving lower permeation rate.

Table 6. Effect of Annealing on RO Performance of 1 Layer of 0.5wt% SPPO-Na on E-500 TFC Membranes

	Annealing conditions		
	None	60°C (5hours)	100°C (0.5hours)
PWP ($x10^{-5}m^3/m^2.s$)	7.2	13.9	2.4
PF ($x10^{-5}m^3/m^2.s$)	6.9	13.8	2.4
$MgSO_4$ Sep% (1500ppm)	72.0±3.4	56.6±5.4	95.1±1.0

Figure 19 shows the effect of annealing on PEG separations of TFC membranes. The MWCO for membrane annealed at 100°C for ½ hour (550) is slightly lower than the membrane with no treatment (around 600), however its average permeate flux during PEG separations was the lowest among the membranes ($2.32x10^{-5}$ $m^3/m^2.s$). On the other hand, membrane annealed at 60°C for 5 hours was observed to have the highest MWCO (around 1000) and a high average permeate flux ($1.3x10^{-4}$ $m^3/m^2.s$). This indicates that the pore sizes of membrane annealed at 60°C were enlarged, whereas those of membrane annealed at 100°C were reduced.

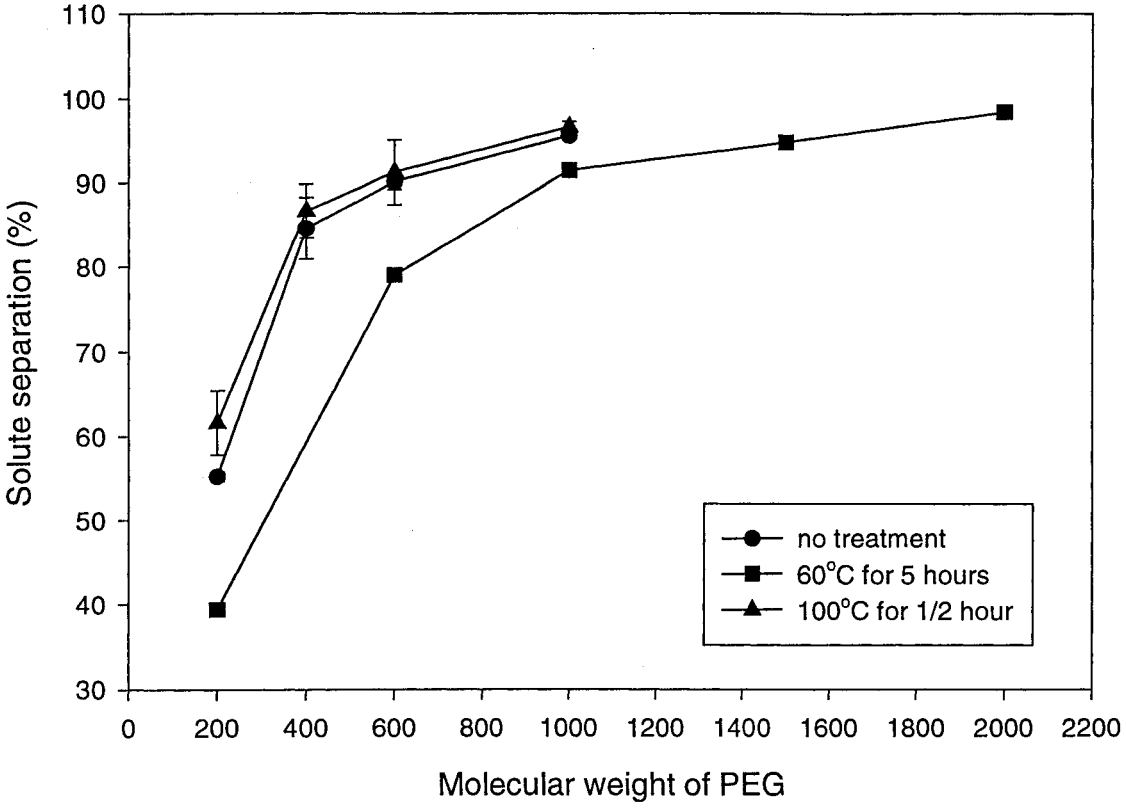

Figure 19. Effect of Annealing on PEG Separation of E-500 Membrane Coated With 1 Layer 0.5wt% SPPO-Na Solution

Figure 20 shows that the slope of the membrane annealed at 100°C for ½ hour is slightly smaller than the slope of membrane without annealing, however, it is still greater than that of membrane annealed at 60°C for 5 hours. The mean pore size of membrane annealed at 100°C for ½ hour is smaller (3.2×10^{-10} m) than those of membrane annealed at 60°C for 5 hours (4.2×10^{-10} m). It can also be concluded that the pore size distribution of the former membrane is more uniform than the latter, confirming the results shown in Figure 19 and Table 6.

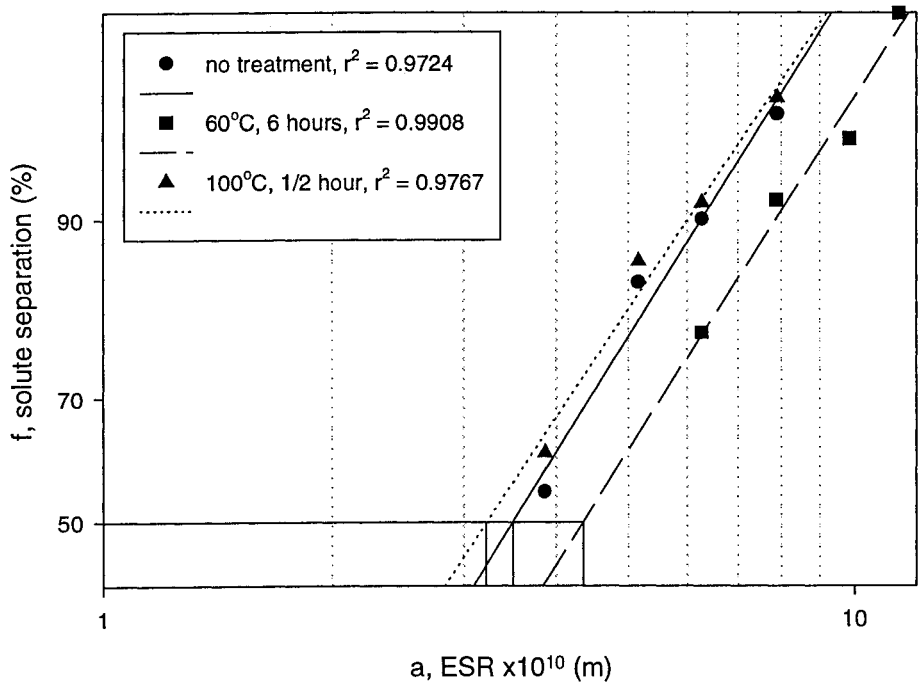

Figure 20. Effect of Annealing on Pore Size and Pore Size Distribution of TFC Membrane (0.5wt% SPPO-Na Coated on E-500)

4.4.2. Effect of heat treatment under water

Another way of heat treatment is to place a membrane in a hot water. This treatment is hereafter called heat treatment under water. This method was described in the experimental part.

Since SPPO is hydrophilic, it was expected that introducing heat treatment under water would increase the permeate flux closer to the desired value. As shown in Table 7, membrane coated with 1 layer of 0.75wt% SPPO-Na without any treatment had a $MgSO_4$ separation of 93.5% which exceeded the goal of 90% separation. However, the permeate flux of this membrane was considered too low ($4.4x10^{-5}$ $m^3/m^2.s$ as compared to goal of $8.7x10^{-5}$ $m^3/m^2.s$). Table 7 shows the comparison of the results with heat treatment for different period for membranes coated with 1 layer of 0.75wt% SPPO-Na.

Table 7. Effect of the Period of Heat Treatment Under Water on RO Performance of TFC E-500 Membranes Coated with 1 Layer of SPPO-Na Having 0.75wt% Concentration

Solute (conc.)	Treatment Period (hr)	PWP ($x10^{-5}m^3/m^2.s$)	PF ($x10^{-5}m^3/m^2.s$)	Separation %
$MgSO_4$	0.0	4.4	4.6	93.5±3.0
(1500ppm)	2.5	1.8	2.0	93.1±3.3
	6.0	8.4	7.2	86.6±1.5

In contrast to annealing, increasing the period of heat treatment under water from 0 to 2.5 hours decreased the pure water permeation rate from $4.4x10^{-5}$ $m^3/m^2.s$ to $1.8x10^{-5}$ $m^3/m^2.s$, while maintaining salt separation of 93%. Increasing the period from 2.5 hours to 6.0 hours, however, increased the pure water permeation to 8.4 $x10^{-5}$ $m^3/m^2.s$ and decreased the salt separation to 87%.

Figure 21 shows the effect of period of heat treatment under water to PEG separations. The PEG separation curves for each membrane, treated or untreated, show a similarity (MWCO around 400 to 500).

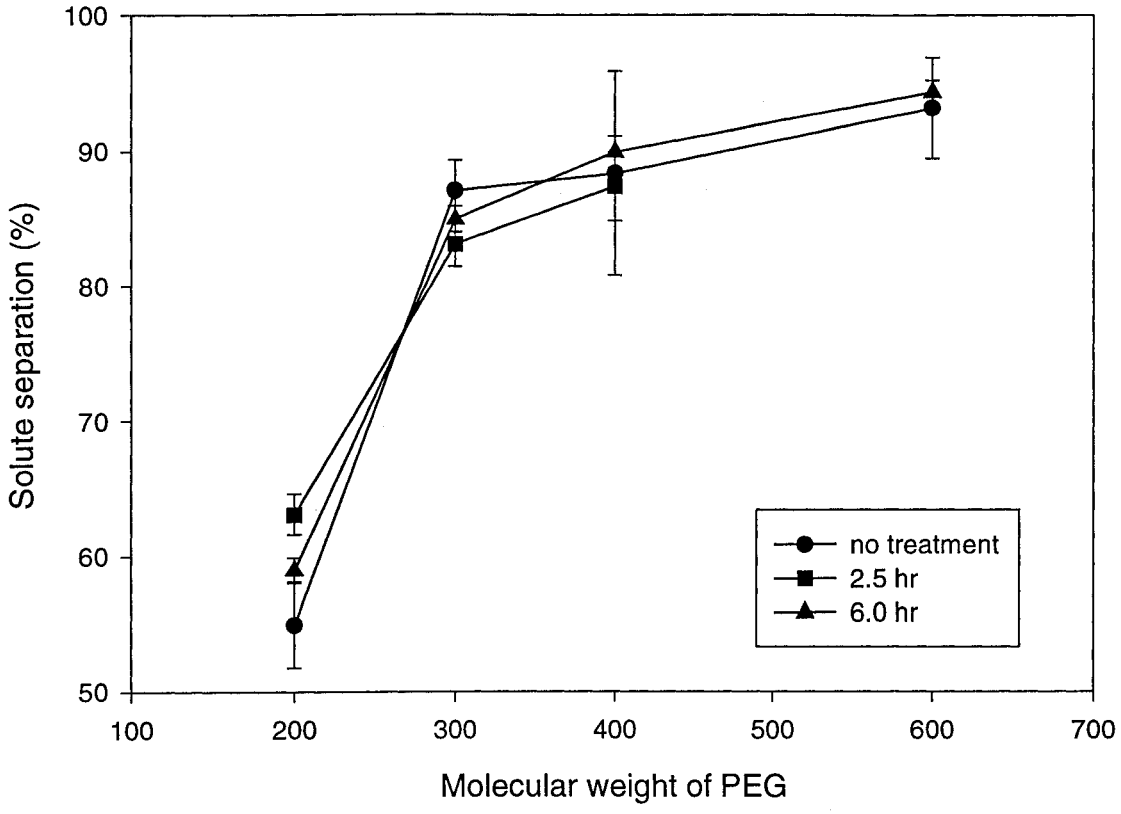

Figure 21. Effect of the Period of Heat Treatment Under Water on MWCO of E-500 Membrane Coated with 1 Layer of 0.75wt% SPPO-Na

Figure 22 shows that the slopes for all membranes were similar. It means the standard deviations of pore sizes for all membranes were similar. The mean pore sizes were also shown to be similar ($3.3x10^{-10}$ m).

It was conjectured that the hydrophilicity of SPPO-Na, as the ultrathin layer of the membranes, is affected by the heat treatment under water. A long period of the treatment is expected to increase the pure water permeation and therefore decrease the electrolyte separation. Thus, when the TFC membrane was exposed to heat treatment under water for

6.0 hours the pure water permeation increased and the electrolyte separation slightly decreased (refer to Table 7). On the other hand, when the TFC membrane was exposed to the treatment only for 2.5 hours, the electrolyte separation was practically unaffected while the pure water permeation decreased.

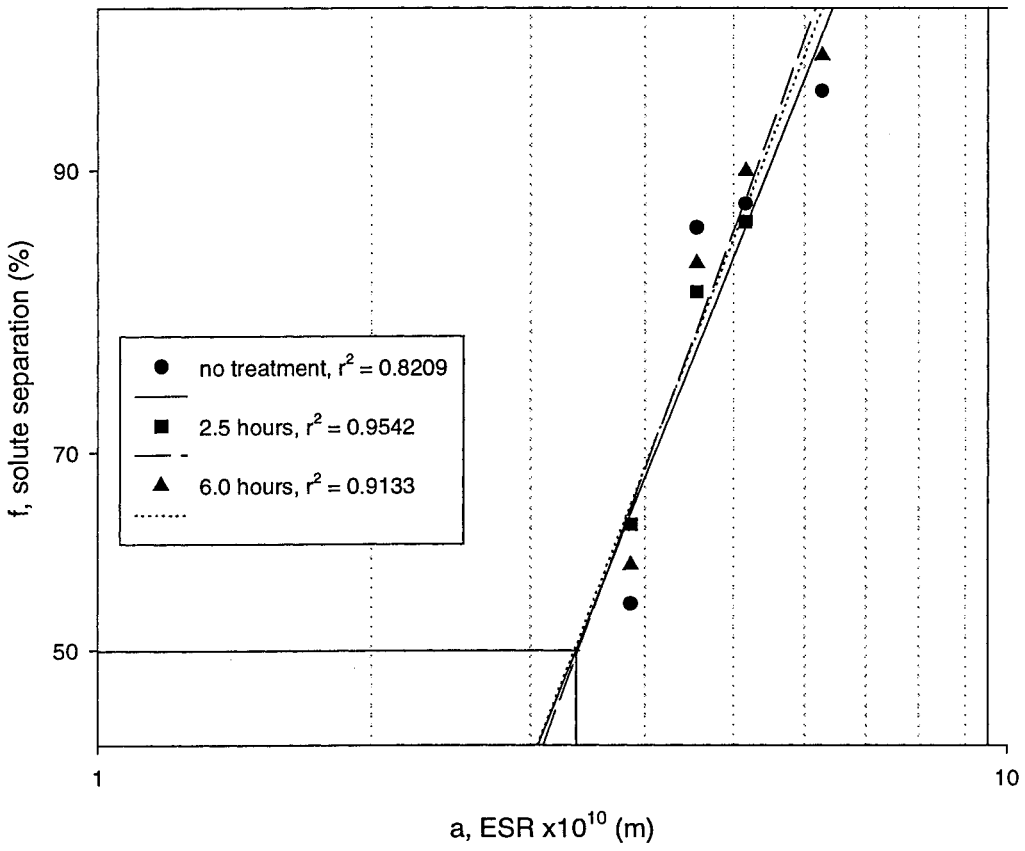

Figure 22. Effect of Heat Treatment Under Water on Pore Size and Pore Size Distribution of TFC Membrane (1 layer of SPPO-Na Having Concentration of 0.75wt% on E-500)

Table 8 summarizes the effect of heat treatment under water on RO performance of E-500 TFC membranes coated with SPPO-Na.

Table 8. Effect of Heat Treatment Under Water on RO Performance of E-500 TFC Membranes

SPPO conc.(wt%)	# of layers	Treatment Period	Salt	PWP (gfd)*	PF (gfd)*	PWP (gfd)*	Sep%	MWCO
0.5	1	0	$MgSO_4$	16.42	15.21	14.06	71.65	600
			NaCl	14.06	18.04	14.50	47.71	
0.5	1	2.5 hr	$MgSO_4$	18.08	17.50	18.94	82.08	400
			NaCl	18.94	18.83	20.10	75.63	
0.5	1	6.0 hr	$MgSO_4$	22.92	22.16	23.80	73.05	500
			NaCl	23.80	23.42	26.77	67.51	
0.5	2	0	$MgSO_4$	17.85	15.15	15.30	74.22	800
			NaCl	15.30	18.15	15.30	84.00	
0.5	2	6.0 hr	$MgSO_4$	24.43	21.45	22.15	84.00	320
			NaCl	22.15	24.50	23.71	73.58	
0.5	3	0	$MgSO_4$	11.15	10.40	11.20	94.09	320
			NaCl	11.20	12.21	13.04	89.88	
0.75	1	0	$MgSO_4$	10.05	10.50	8.80	93.51	350
			NaCl	8.80	9.93	8.73	77.39	
0.75	1	2.5 hr	$MgSO_4$	4.24	4.46	4.68	93.14	350
			NaCl	4.68	4.62	4.52	86.63	
0.75	1	6.0 hr	$MgSO_4$	19.30	16.63	17.71	86.62	350
			NaCl	17.70	19.81	18.07	74.82	
0.75	2	6.0 hr	$MgSO_4$	26.53	25.48	26.68	77.85	500
			NaCl	26.68	27.76	29.98	77.88	
1.00	1	0	$MgSO_4$	5.10	4.53	5.10	71.73	-
			NaCl	5.10	5.03	5.10	51.05	
1.00	1	1.0 hr	$MgSO_4$	2.13	2.25	2.24	92.66	300
			NaCl	2.24	2.37	2.11	88.39	
1.00	1	2.5 hr	$MgSO_4$	2.55	2.33	2.35	92.26	300
			NaCl	2.35	2.55	2.34	89.62	
1.00	1	6.0 hr	$MgSO_4$	11.64	11.33	11.66	61.83	450
			NaCl	11.66	11.71	11.27	74.37	
1.00	2	6.0 hr	$MgSO_4$	15.88	14.88	15.22	71.12	450
			NaCl	15.22	15.97	17.45	83.59	

* 1 gfd = 4.3×10^{-6} $m^3/m^2.s$

From all the results presented, it can be concluded that the goal of having a membrane with $MgSO_4$ separation of 90% and permeation rate of 8.73 x 10^{-5} $m^3/m^2.s$ was almost achieved by the membrane having 1 layer of 0.75wt% coating on E-500 substrate membrane which was heat treated under water. The performance of this membrane was $MgSO_4$ separation of 87% and permeation rate of 8.4 x10^{-5} $m^3/m^2.s$. Should $MgSO_4$ separation of greater than 90% be strongly urged, then permeation rate must be sacrificed. In this case, the membrane of the same coating without heat treatment would satisfy the aim, with $MgSO_4$ separation of 93.5%. However, the permeation rate for this membrane would be 4.4 x10^{-5} $m^3/m^2.s$.

CHAPTER FIVE

CONCLUSION

From the results and discussions of this work, the following conclusions can be drawn:

1. Polyethersulfone material proved to be a better substrate membrane in the preparation of thin film composite membrane compared to polyvinylidene material in terms of permeation rate and selectivity.

2. Increasing the number of coating layer increased solute separation, however, decreased the permeation. Thus, one layer of coating was concluded as the optimum condition.

3. Increasing the coating solution concentration initially increased the solute separation, but later decreased the solute separation. Coating solution concentration of 0.75wt% was concluded to have the optimum solute separation.

4. When heat treatment period was longer than 5 hours, both annealing and heat treatment under water increased the permeation rate and decreased the $MgSO_4$ separation. However, the decrease of the $MgSO_4$ separation in annealing was twice as much as that in heat treatment under water. Thus, heat treatment under water was concluded to more support attaining the targeted value.

5. The targeted solute separation and permeation rate were considered to be achieved when commercial E-500 ultrafiltration membrane was coated with 1 layer of 0.75 wt% SPPO-Na in methanol, followed by heat treatment under water.

Recommendation

It is recommended that further study for post-treatment of TFC membranes with heat treatment under water is conducted to better understand the phenomena of low pure water permeation under short period of the treatment. Pilot scale of this work is also recommended to further confirm the results obtained.

References

Agarwal, A. K. and R. Y. M. Huang, "Development and Transport Properties of Novel Sulfonated Poly (Phenylene Oxide) Thin-Film Composite Charged Ultrafiltration Membranes for Bioseparations", Angew. Makromol. Chem., **163**, 1, (1988)

Brandt, D. C., G. F. Leitner and W. E. Leitner "Reverse Osmosis Membranes State of The Art", in Reverse Osmosis, Amjad, Z., ed., Van Nostrand Reinhold, New York, N.Y., 1-36, (1993)

Cadotte, J. E. and R. J. Petersen, "Thin-Film Composite RO Membranes : Origin, Development, and Recent Advances", Synthetic Membranes, Vol. I, Desalination, ACS Symposium Series, **153**, 305-321, (1981)

Cabasso, I., J. J. Grodzinski and D. Vofsi, "Synthesis and Characterization of Polymers with Pendent Phosphonate Groups", J. Appl. Polym. Sci., **18**, 1969-1986, (1974)

Chludzinski, P., J. F. Austin and J. Enos, "Development of Polyphenylene Oxide Membranes", Research and Development Progress Report no. 697, US Department of Interior, June 1971

Chowdhury, G., T. Matsuura and S. Sourirajan, "A Study of Reverse Osmosis Separation and Permeation Rate for Sulfonated Poly(2,6-dimethyl-1,4-phenylene oxide) Membranes in Different Cationic Forms", J. Appl. Polym. Sci., **51**, 1071-1075, (1994)

Dohany, J. E. and H. Stefanou, Am. Chem. Soc. Div. Org. Coating Plastic Chemistry Paper, **35**(2), 83, (1975)

Dohany, J. E. and J. S. Humprey, "Vinylidene Fluoride Polymers", in Encyclopedia of Polymer Science and Engineering, Hay, A. S., 2nd ed., Wiley & Sons, New York, N.Y., **17**, 532-548, (1985)

Francis, P. S., "Fabrication and Evaluation of New Ultrafiltration Reverse Osmosis Membranes", National Technical Information Service, Springfield, VA, Report #PB-177083, (1966)

Fu, H., L. Jia and J. Xu, "Studies on the Sulfonation of Poly (phenylene oxide) (PPO) and Permeation Behavior of Gases and Water Vapor Through Sulfonated PPO Membranes. I. Sulfonation of PPO and Characterization of the Products", J. Appl. Polym. Sci., **51**, 1399-1404 (1994)

Gilbert, E. E., "Sulfonation and Related Reactions", Interscience Publishers, a division of John Wiley & Sons, New York, N.Y., (1965)

Hamza, A., G. Chowdhury, T. Matsuura, S. Sourirajan, " Study of Reverse Osmosis Separation and Permeation Rate for Sulfonated Poly(2,6-dimethyl-1,4-phenylene oxide) Membranes of Different Ion Exchange Capacities", J. Appl. Polym. Sci., **58**, 613-620, (1995)

Harris, J. E. and R. M. Johnson, "Polysulfones", in Encyclopedia of Polymer Science and Engineering, Hay, A. S., 2nd ed., Wiley & Sons, New York, N.Y., **13**, 196-211, (1985)

Hay, A. S., "Sulfonation and Sulfation", Encyclopedia of Polymer Science and Engineering, 2nd ed., Wiley & Sons, New York, N.Y., **10**, 1-41, (1969)

Helfferich, F., "Ion Exchange", McGraw-Hill, New York, N.Y., 134-140, (1962)

Hertzberg, R. W. and J. A. Manson, "Fatigue of Engineering Plastics", Academic Press, Orlando, F.A., (1980)

Ikeda, K., T. Nakano, H. Ito, T. Kubota and S. Yamamoto, "New Composite Charged Reverse Osmosis Membrane", Desalination, **68**, 109-119, (1988)

Ishiguro, M., T. Matsuura and C. Detellier, " A Study on the Solute Separation and the Pore Size Distribution of a Montmorillonite Membrane", Sep. Sci. Technol. , **31**, 545-556, (1996)

Jitsuhara, I., and S. Kimura, "Structure and Properties of Charged Ultrafiltration Membrane Made of Sulfonated Polysulfone", J. Chem. Eng. Japan, **16**, 389-393, (1983)

Kambour, R. P., E. E. Romagosa and C. L. Gruner, "Swelling, Crazing and Cracking of An Aromatic Copolyethersulfone in Organic Media", Macromolecules, **5**, 335-340, (1972)

Kemper, W. D. and D. E. L. Maasland, "Reduction in Salt Content of Solution on Passing Through Thin Films Adjacent to Charged Surfaces", Soil Science Society of America Proceedings, **28**, 318-323, (1964)

Kurihara, M., T. Uemura, N. Nakagawa and T. Tonomura, "The Thin-Film Composite Low Pressure Reverse Osmosis Membranes", Desalination, **54**, 75-88, (1985)

Matsuura, T., "Synthetic Membranes and Membrane Separation Processes", CRC Press, Boca Raton, F.A., (1994)

Michaels, A. S., "Analysis and Prediction of Sieving Curves for Ultrafiltration Membranes : A Universal Correlation ?", Sep. Sci. Technol., **15**, 1305-1321, (1980)

Mulder, M. H. V., "Basic Principles of Membrane Technology", Klumer Academic, Boston, M. A., (1992)

Nakao, S., H. Osada, H. Kurata, T. Tsuru and S. Kimura, "Separation of Proteins by Charged Ultrafiltration Membranes", Desalination, **70**, 191-195, (1988)

Percec, S., "Chemical Modification of Poly (2,6-Dimethyl-1,4-Phenylene Oxide) by Friedel Crafts Reactions", J. Appl. Polym. Sci., **33**, 191-203, (1987)

Percec, V. and B. C. Auman, "Phase Transfer Catalysis. Functional Polymers and Sequential Copolymers by Phase Transfer Catalysis. 5. Synthesis and Characterization of Polyformals of Aromatic Polyethersulfones", Polymer Bulletin, Berlin, **10**, 385-390, (1983)

Petersen, R. J., "Composite Reverse Osmosis and Nanofiltration Membranes", J. Membrane Sci., **83**, 81-150, (1993)

Plummer, C. W., G. Kimura and A. B. La Conti, "Development of Sulfonated Polyphenylene Oxide Membrane for Reverse Osmosis", Research and Development Progress Report #551, Office of Saline Water, US Department of Interior, May 1970

Riley, R. L., H. K. Lonsdale, L. D. La Grange and C. R. Lyons, "Development of Ultrathin Membranes", NTIS Report No. PB-207036, (Jan 1969)

Riley, R. L., H. K. Lonsdale and C. R. Lyons, "Composite Membranes for Seawater Desalination by Reverse Osmosis", J. Appl. Polym. Sci., **15**, 1267-1276, (1971)

Riley, R. L., J. O. Gardner and U. Merten, "Cellulose Acetate Membranes: Electron Microscopy of Structure", Science, **143**, 801-803, (1964)

Robeson, L. M. and S. T. Crisafulli, "Microcavity Formation in Engineering Polymers Exposed to Hot Water", J. Appl. Polym. Sci., **28**, 2925-2936, (1983)

Rolfe, P. F. and L. A. G. Aylmore, "Water and Salt Flow Through Compacted Clays. II. Electrokinetics and Salt Sieving", J. Colloid Interface Sci., **79**, No. 2, 301-307, (1981)

Rozelle, L. T., J. E. Cadotte, R. D. Cornelliussen and E. E. Erickson, "Final Report on Development of New Reverse Osmosis Membranes", National Technical Information Service, Springfield, VA, Report #PB-206329, (1967)

Rozelle, L. T., J. E. Cadotte, K. E. Kobian and C. V. Kopp Jr., "Nonpolysaccharide Membranes for Reverse Osmosis : NS-100 Membranes", in Reverse Osmosis and Synthetic Membranes, Sourirajan, S. ed., National Research Council, Ottawa, p.249-255, (1977)

Sata, T. and R. Izuo, "Modification of Transport Properties of Ion Exchange Membrane. XI. Electrodialytic Properties of Cation Exchange Membranes Having Polyethyleneimine Layer Fixed by Acid-Amide Bonding", J. Appl. Polym. Sci., **41**, 2349-2362, (1990)

Sata, T., R. Yamane and Y. Mizutani, "Modification of Transport Properties of Ion Exchange Membrane. VII. Relative Transport Number between Various Cations of Cation Exchange Membrane Having Cationic Polyelectrolyte Layer and Mechanism of Selective Permeation of Particular Cations", J. Appl. Polym. Sci., Polym. Chem. Ed., **17**, 2071-2085, (1979)

Schauer, J., P. Lopour and J. Vacik, " The Preparation of Ultrafiltration Membranes from a Moderately Sulfonated Poly(oxy(2,6-dimethyl-1,4-phenylene))", J. Membrane Sci., **29**, 169-175, (1986)

Schnoor, W. G. and A. W. Yodis, U.S. Pat. 3,160,474, (1964)

Sirkar, K. K. and W. S. W. Ho, "Membrane Handbook", Van Nostrand Reinhold, New York, N.Y., p. 411-421, (1992)

Sourirajan, S., "Reverse Osmosis and Synthetic Membranes", National Research Council Canada, Ottawa, p.211-235, (1977)

Sourirajan, S. and T. Matsuura, "Reverse Osmosis and Ultrafiltration", American Chemical Society, Washington D.C., p. 21-32, (1985)

Standen, A., Encyclopedia of Chemical Technology, 2nd ed., **16**, John Wiley & Sons, New York, N.Y., (1968)

Tsuru, T., M. Urairi, S. Nakao and S. Kimura, "Reverse Osmosis of Single and Mixed Electrolytes with Charged Membranes: Experimental and Analysis", J. Chem. Eng. Japan, **24**, 518-524, (1991)

Verdet, L., and J. K. Stille, "Poly (phenylene oxide) Catalyst Supports Containing (Cyclo Pentadiene) Metal Complexes", Organometallics, **1**, 380-384, (1982)

Xie, S., W. J. MacKnight, and F. E. Karasz, J. Appl. Polym. Sci., Part A-1, **7**, 691-698, (1968)

Zhou, Q.H., S. Sourirajan and T. Matsuura, "A Transport Model for Reverse Osmosis Separation of Binary Organic Liquid Mixtures", Chem. Eng. Commun., **104**, 177-208, (1991)

APPENDIX A
SAMPLE CALCULATIONS

I. Permeate flux (PF)

Using raw data for SPPOH-PES composite membrane, prepared from coating solution of 1.0wt% SPPOH, with magnesium sulfate feed solution.

The permeate flux is calculated as follows:

$$PR = \left(\frac{V}{A \times t} \right) \times T_C$$

Where V is the volume permeating the membrane of area A in time t and T_c is the temperature-correcting factor (from temperature T°C to temperature 25°C) estimated based on pure water properties as :

$$T_C = \left(\frac{\mu_{T^\circ C}}{\mu_{25^\circ C}} \right) \left(\frac{\rho_{25^\circ C}}{\rho_{T^\circ C}} \right)$$

The water density and viscosity values were taken from "Lange's Handbook of Chemistry", J.A. Dean Ed., McGraw-Hill Company, Thirteen Edition (1985).

Operating temperature was 27°C. Water properties are :

$\mu_{25}{}^\circ C = 0.894 \times 10^{-3}$ N.s/m^2 $\quad$ $\mu_{27}{}^\circ C = 0.855 \times 10^{-3}$ N.s/m^2

$\rho_{25}{}^\circ C = 997.0$ kg/m^3 $\quad$ $\rho_{27}{}^\circ C = 996.5$ kg/m^3

Thus, the temperature correction factor is :

$$T_c = 0.957$$

From the Appendix G, the permeate rate from AP-10 membrane cell 1 and cell 2 are 0.772 and 0.836, respectively, resulting in an average of V = 0.804 mL/min. Each membrane area A = 10.2 cm^3.

Thus, the average permeate flux is :

$$PF = 14.1 \times 10^{-5}\ m^3/m^2.s$$

In the range of salt concentrations studied, the relationship between the solution concentration and its conductivity is linear enabling direct calculations of solute separation from conductivity measurements (refer to Appendix D).

II. Solute separation

The solute separation is calculated as follows:

$$f = \frac{C_f - C_p}{C_f} \times 100\%$$

Where C_p is the solute concentration in the permeate and C_f is the solute concentration in the feed.

During the AP-10 membrane substrate experiment, feed conductivity changed from initial value of 1.98 mS/cm to a final value of 1.94 mS/cm, giving an average C_f = 1.96 mS/cm (refer to Appendix F). The permeate conductivity through the two membranes were 1.62 and 1.66 mS/cm, resulting in an average of C_p 1.64 mS/cm.

Thus, the average fractional magnesium sulfate separation is

$$f = (1.96 - 1.64)/1.96 \times 100\%$$

$$f = 16.4\%$$

III. Ion exchange capacity (IEC) value

0.567 g of SPPO-H polymer was dissolved in 25 mL of 1 N NaOH. The solution was left overnight after being covered with a parafilm. The solution was then titrated with HCl. The amount of NaOH, which did not react with the polymer, reacted with HCl on one to one ratios and was labeled as x. Therefore, the amount of NaOH that reacted with the polymer will be (25-x) mL. The amount of HCl used for titration was calculated to be 14.6 mL. Thus, x = 14.6 mL. The IEC is then calculated as follow:

$$IEC = \frac{(25-x)}{w} \times N$$

where : x = amount of NaOH which did not react with the SPPO polymer

w = weight of the SPPO polymer

N = normality of NaOH

Using the values available, IEC value is calculated to be:

$$IEC = \frac{(25-14.6)}{0.567} \times 0.1$$

$$IEC = 1.867 \qquad \text{meq / g dry polymer}$$

IV. Molecular weight cut off (MWCO)

Using the PEG separation data for HW-18 substrate membrane in the appendix B, the separation data for MW of 3400 was 88.81%, whereas the separation data for MW of 8000 was 95.38%. The MWCO is then calculated using linear interpolation as follows:

$$\frac{MWCO - 2000}{8000 - 2000} = \frac{90.00 - 89.09}{95.38 - 89.09}$$

$$MWCO = 2868.04$$

Because MWCO is always an average value, then MWCO is taken as 2900.

APPENDIX B

Experimental Reverse Osmosis Performance Data

I. PEG separation and permeate flux for substrate membranes

	E-500		HW-18		AP-10	
MW of PEG	Separation (%)	PF ($m^3/m^2.s$)	Separation (%)	PF ($m^3/m^2.s$)	Separation (%)	PF ($m^3/m^2.s$)
200	12.05	0.000191	18.45	0.000118	9.946667	0.000380
400	-	-	-	-	21.54333	0.000341
600	44.25	0.000243	51.81	0.000131	25.30667	0.000386
1000	67.22	0.000221	81.11	0.000139	32.85000	0.000354
1500	74.98	0.000229	83.44	0.000136	41.86667	0.000377
2000	80.30	0.000224	89.09	0.000114	48.32570	0.000385
3400	87.47	0.000149	88.81	0.000110	62.92587	0.000394
4000	87.38	0.000151	-	-	70.05811	0.000397
6000	-	-	-	-	80.23540	0.000367
7500	90.83	0.000156	-	-	-	-
8000	-	-	95.39	0.000115	89.99985	0.000377

II. PEG separation and permeate flux for TFC membranes, each coated with 1 layer of 1.0wt% SPPO-H

	Coated E-500		Coated HW-18		Coated AP-10	
MW of PEG	Separation (%)	PF ($m^3/m^2.s$)	Separation (%)	PF ($m^3/m^2.s$)	Separation (%)	PF ($m^3/m^2.s$)
200	44.71	0.000100	41.45	0.0000680	22.205	0.000163
400	-	-	-	-	42.265	0.000150
600	84.13	0.000101	84.45	0.0000627	58.665	0.000158
1000	92.56	0.000114	89.29	0.0000568	73.630	0.000140
1500	95.56	0.000106	95.52	0.0000602	85.330	0.000153
2000	96.63	0.000095	96.60	0.0000668	90.470	0.000137
3400	97.24	0.000090	-	-	95.630	0.000156
4000	-	-	-	-	95.470	0.000154
6000	-	-	-	-	98.965	0.000148
8000	98.56	0.000094	-	-	-	-

III. PEG separation for E-500 membrane coated with SPPO-Na of 0.5wt% concentration with different number of layers

MW of PEG	Solute separation (%)		
	1 layer	2 layers	3 layers
200	55.15	43.93	52.17
300	-	-	74.29
400	84.58	67.59	78.71
600	90.05	76.92	91.83
900	94.14	-	-
1000	95.82	90.12	-
1500	-	93.06	-

IV. PEG separation for E-500 membrane coated with 1 layer of SPPO-Na with different concentrations

MW of PEG	Solute separation (%)	
	0.5wt%	0.75wt%
200	55.15	54.92
300	-	87.03
400	84.58	88.32
600	90.05	93.20
900	94.14	-
1000	95.82	-
1500	-	-

V. PEG separation for E-500 membrane coated with 1 layer of 0.5wt% SPPO-Na treated with different annealing temperature and period

MW of PEG	Solute separation (%)		
	Not annealed	60oC 6 hours	100oC ½ hour
200	55.15	39.43	61.58
300	-	-	-
400	84.58	-	86.63
600	90.05	78.96	91.19
900	94.14	-	95.00
1000	95.82	91.42	96.40
1500	-	94.79	-

VI. PEG separation for E-500 membrane coated with 1 layer of 0.75wt% SPPO-Na subjected to heat treatment under water at 84°C with different period

MW of PEG	Solute separation (%)		
	Not treated	2.5 hours	6 hours
200	54.92	63.09	58.95
300	87.03	83.07	84.94
400	88.32	87.37	89.94
600	93.20	-	94.36

APPENDIX C

Correction Factor for Permeate Flux for Temperature of 25°C

Temperature (°C)	Density (kg/m^3)	Viscosity (cP)	Factor (T_c)
15	999.099	1.1404	1.2734
16	998.943	1.1111	1.2409
17	998.775	1.0828	1.2095
18	998.595	1.0559	1.1797
19	998.405	1.0299	1.1508
20	998.204	1.0050	1.1232
21	997.992	0.9810	1.0966
22	997.770	0.9579	1.0711
23	997.538	0.9358	1.0466
24	997.296	0.9142	1.0227
25	997.045	0.8937	1.0000
26	996.783	0.8737	0.9779
27	996.513	0.8545	0.9566
28	996.233	0.8360	0.9362
29	995.945	0.8180	0.9163
30	995.645	0.8007	0.8972
31	995.341	0.7840	0.8788
32	995.026	0.7679	0.8610
33	994.703	0.7523	0.8438
34	994.371	0.7371	0.8270
35	994.032	0.7225	0.8109

APPENDIX D

Calibration Curve Relating Conductance to Concentration of $MgSO_4$

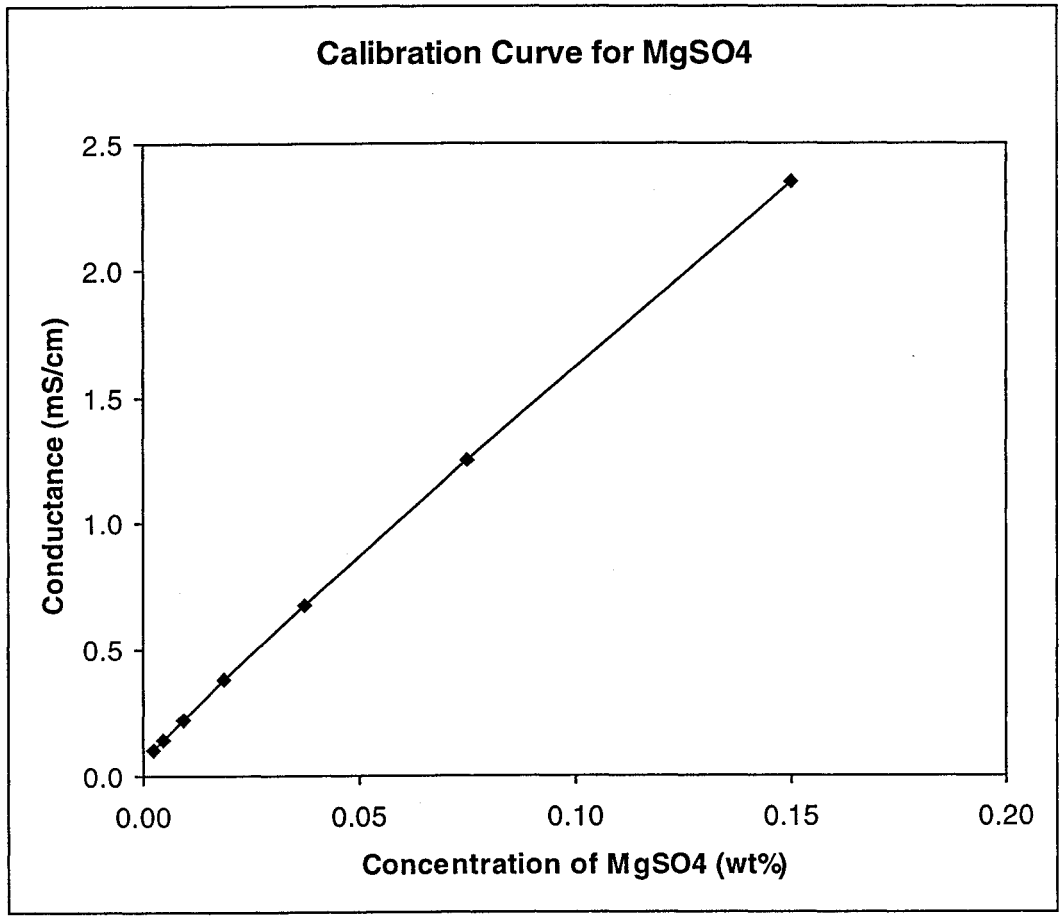

APPENDIX E

NMR Study of SPPO-Na

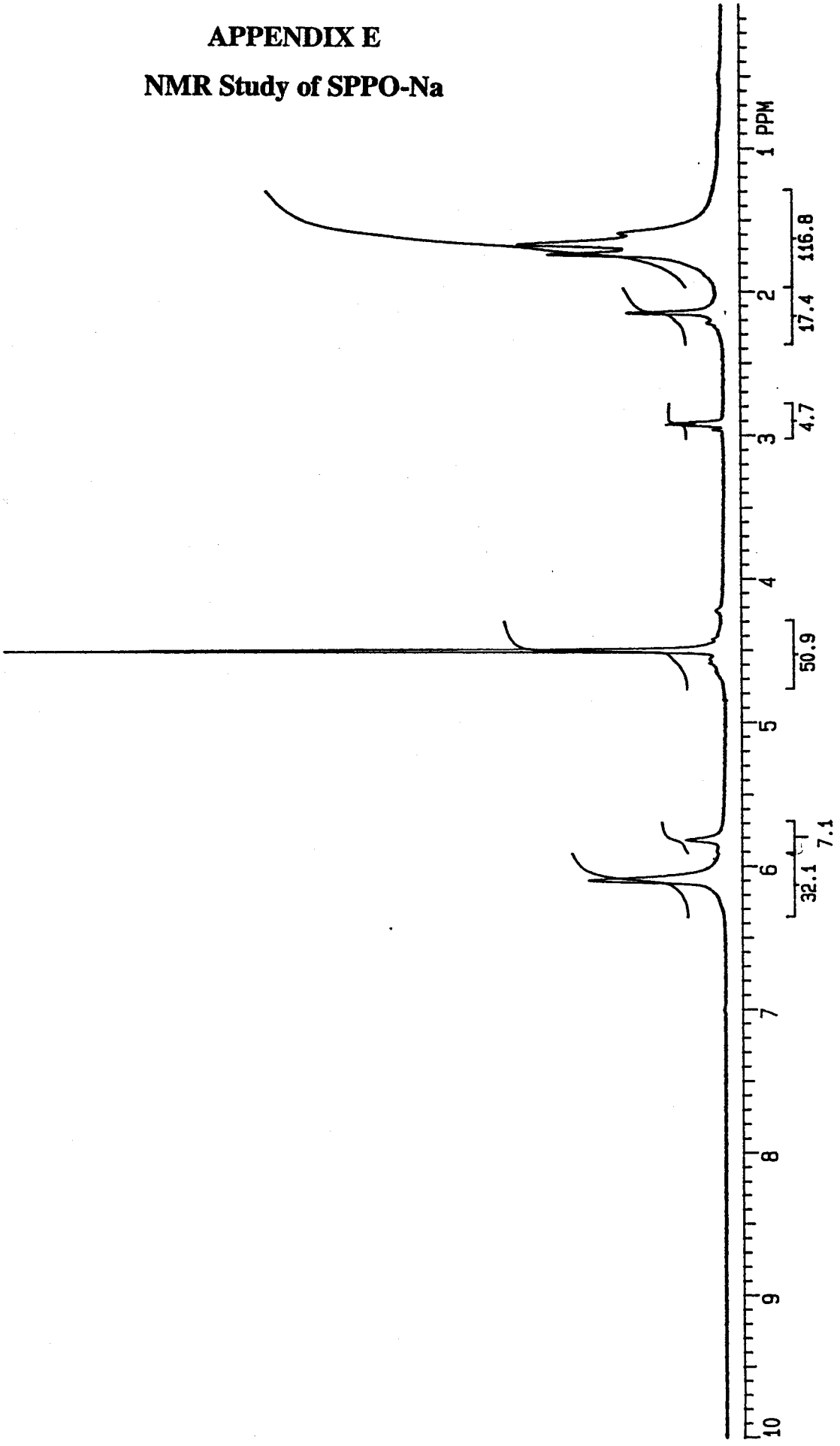

APPENDIX F

RAW DATA FOR CONDUCTIVITY

Substrate membrane	Number of coating	Coating concentration	Heat treated	Separation (%)	Conductivity (mS/cm)		
					Cell 1	Cell 2	Feed
AP-10	-	-	-	16.4	1.62	1.66	1.96
	1, SPPOH	1.0wt%	-	38.0	1.12	1.31	1.96
HW-18	-	-	-	27.4	1.40	1.38	1.91
	1, SPPOH	1.0wt%	-	69.6	0.70	0.63	2.17
E-500	-	-	-	23.0	1.43	1.51	1.91
	1,SPPOH	1.0wt%	-	59.1	0.90	0.87	2.17
	1,SPPONa	0.5wt%	-	72.0	0.53	0.56	1.93
	2,SPPONa	0.5wt%	-	74.2	0.47	0.53	1.93
	3,SPPONa	0.5wt%	-	89.0	0.19	0.26	2.08
	1,SPPONa	0.75wt%	-	93.5	0.15	0.14	2.08
	1,SPPONa	1.0wt%	-	71.7	0.58	0.60	2.07
	1,SPPONa	0.5wt%	an,60°C^{+}	56.6	0.88	0.87	2.01
	1,SPPONa	0.5wt%	an,100°C^{+}	95.1	0.1	0.9	2.01
	1,SPPONa	0.75wt%	2.5hrboil*	93.1	0.12	0.17	2.04
	1,SPPONa	0.75wt%	6.0hrboil*	86.6	0.35	0.30	2.37

Note : boil* = heat treatment under water

an^{+} = annealing

APPENDIX G

RAW DATA FOR PERMEATE FLUX

Substrate Membrane	Number of coating	coating conc.	heat treatment	Permeate rate (ml/min)			temp (°C)	Tc	PF ($m^3/m^2.s$)
				cell1	cell2	average			
AP-10	-	-	-	1.709574	1.888263	1.798919	25.00	1.000601	30
	1,SPPOH	1.0wt%	-	0.77197	0.83599	0.80398	22.80	1.052265	14.1
HW-18	-	-	-	0.713969	0.696963	0.705466	25.60	0.986582	11.6
	1,SPPOH	1.0wt%	-	0.376214	0.380923	0.378568	21.70	1.077745	6.8
E-500	-	-	-	1.029224	0.98658	1.007902	26.10	0.976285	16.4
	1,SPPOH	1.0wt%	-	0.561181	0.607227	0.584204	21.70	1.078391	10.5
	1,SPPONa	0.5wt%	-	0.397902	0.392774	0.395338	23.30	1.039616	6.85
	2,SPPONa	0.5wt%	-	0.436779	0.415719	0.426249	28.20	0.933257	6.63
	3,SPPONa	0.5wt%	-	0.277817	0.272114	0.274966	25.10	0.999398	4.58
	1,SPPONa	0.75wt%	-	0.301389	0.26178	0.281585	26.10	0.975905	4.58
	1,SPPONa	1.0wt%	-	0.118515	0.133428	0.125971	27.70	0.943071	1.98
	1,SPPONa	0.5wt%	an,60oC+	0.804752	0.850013	0.827382	24.90	1.002197	13.82
	1,SPPONa	0.5wt%	an,100oC+	0.136462	0.13191	0.134186	21.20	1.09102	2.44
	1,SPPONa	0.75wt%	2.5hrboil*	0.143814	0.08937	0.116592	24.60	1.008644	1.96
	1,SPPONa	0.75wt%	6.0hrboil*	0.426445	0.435079	0.430762	24.70	1.008446	7.24